Copyright Warning & Restrictions

The copyright law of the United States (Title 17, United States Code) governs the making of photocopies or other reproductions of copyrighted material.

Under certain conditions specified in the law, libraries and archives are authorized to furnish a photocopy or other reproduction. One of these specified conditions is that the photocopy or reproduction is not to be "used for any purpose other than private study, scholarship, or research." If a, user makes a request for, or later uses, a photocopy or reproduction for purposes in excess of "fair use" that user may be liable for copyright infringement,

This institution reserves the right to refuse to accept a copying order if, in its judgment, fulfillment of the order would involve violation of copyright law.

Please Note: The author retains the copyright while the New Jersey Institute of Technology reserves the right to distribute this thesis or dissertation

Printing note: If you do not wish to print this page, then select "Pages from: first page # to: last page #" on the print dialog screen

ABSTRACT
LABORATORY STUDIES OF THE BIODEGRADATION OF CHEMICALLY DISPERSED OIL: EFFECT OF DROPLET SIZE AND NUTRIENT AMENDMENT

by
Christopher D'Ambrose

Oil spills could have devastating effects on the shorelines, and for this reason, chemical dispersants are commonly used to disperse the oil slick in the water column, preventing it from reaching the shorelines. However, the long term fate of dispersed oil depends on its biodegradation by indigenous microorganisms, which in turn depends on the concentration of nutrients in water and on the droplet size distribution.

Using water from the shorelines of Atlantic City, we placed the water with oil and dispersant inside EPA Baffled Flasks and placed them on rotatory shakers. We selected two speeds: high (250 rpm) and low (125 rpm). We also added excess nutrient for some of the flasks to evaluate the role of nutrient. The experiments reflected the following situations: HSHN, HSLN, LSHN, and C, where HS and LS mean high (250 rpm) and low (125 rpm) speed mixing, respectively. HN and LN means high and low nutrient, respectively. C means control, which was HSLN with azide added to inhibit bacterial activity, and subsequently oil biodegradation. The initial median oil droplet was 3.00 microns, 3.15 microns, 4.34 microns, and 3.48 microns for the HSHN, HSLN, LSHN, and C, respectively. The biodegradation rates for HSHN, HSLN, LSHN was 82%, 87%, and 51% respectively. Thus, smaller droplet sizes promoted the biodegradation of oil.

LABORATORY STUDIES OF THE BIODEGRADATION OF CHEMICALLY DISPERSED OIL: EFFECT OF DROPLET SIZE AND NUTRIENT AMENDMENT

by
Christopher D'Ambrose

A Dissertation
Submitted to the Faculty of
New Jersey Institute of Technology
in Partial Fulfillment of the Requirements for the Degree of
Doctor of Philosophy in Chemical Engineering

Otto H. York Department of
Chemical, Biological and Pharmaceutical Engineering

January 2016

.

APPROVAL PAGE

LABORATORY STUDIES OF THE BIODEGRADATION OF CHEMICALLY DISPERSED OIL: EFFECT OF DROPLET SIZE AND NUTRIENT AMENDMENT

Christopher D'Ambrose

Dr. Michel Boufadel, Dissertation Co-Advisor Date
Professor of Civil and Environmental Engineering, NJIT

Dr. Norman Loney, Dissertation Co-Advisor Date
Professor of Chemical, Biological and Pharmaceutical Engineering, NJIT

Dr. Piero M. Armenante, Committee Member Date
Distinguished Professor of Chemical, Biological and Pharmaceutical Engineering, NJIT

Dr. Robert B. Barat, Committee Member Date
Professor of Chemical, Biological and Pharmaceutical Engineering, NJIT

Dr. Laurent Simon, Committee Member Date
Associate Professor of Chemical, Biological and Pharmaceutical Engineering, NJIT

Dr. Wen Zhang, Committee Member Date
Assistant Professor of Civil and Environmental Engineering, NJIT

BIOGRAPHICAL SKETCH

Author: Christopher D'Ambrose

Degree: Doctor of Philosophy

Date: January 2016

Undergraduate and Graduate Education:

- Doctor of Philosophy in Chemical Engineering,
  New Jersey Institute of Technology, Newark, NJ, 2016
- Master of Engineering in Chemical Engineering,
  The Cooper Union, New York, NY, 2010
- Bachelor of Engineering in Chemical Engineering,
  The Cooper Union, New York, NY, 2008

Major: Chemical Engineering

Presentations and Publications:

D'Ambrose, Christopher; Pan, Zhong; Boufadel, Michel C., "Laboratory Studies of the Biodegradation of Chemically Dispersed Oil: Effect of Droplet Size and Nutrient Amendment," Manuscript in progress.

Yi, Shize; Zhao, Lin; D'Ambrose, Christopher; Boufadel, Michel C., "Effects of Mixing Energy and Time on the Dispersibility of Crude Oil in Sea Water," Manuscript in progress.

Zhao, Lin; Shaffer, Franklin; Robinson, Brian; King, Thomas; D'Ambrose, Christopher; Pan, Zhong; Miller, Richard; Conmy, Robyn; Boufadel, Michel,C., "Underwater oil jet: Hydrodynamics and droplet size distribution," Environmental Science & Technology, Manuscript submitted for publication.

I would like to dedicate this dissertation to the loving memory of my father;

Joseph Robert D'Ambrose

ACKNOWLEDGMENT

I would like to thank my PhD co-advisers; Dr. Michel Boufadel and Dr. Norman Loney. Dr. Boufadel provided me with the opportunity and technical background to complete this dissertation. Dr. Loney supported me during my entire duration here at NJIT. I would also like to thank my committee members for all of their assistance and guidance through this long process: Dr. Piero Armenante, Dr. Robert Barat, Dr. Laurent Simon, and Dr. Wen Zhang.

I also appreciate all of the help from everyone at the NRDP Center, including Dr. Xiaolong Geng and Dr. Zhong Pan, as well as all of the other post docs, graduate students, and undergrads who I have worked with.

I would like to thank the sources for my funding: Linger Exxon Valdez Spill, Fisheries and Oceans Canada, Solidifying the Scientific Capabilities of Ohmsett - Wave Hydrodynamics (Topic 7), and the National Oceanic and Atmospheric Administration.

I would also like to thank all of my peers who contributed with their advice and support. Thanks to my friends who have supported me while I was working on this PhD. Lastly, thanks to all of my family members, including my siblings, parents, grandparents, and cousins who have always been there for me while I was working on this PhD and throughout all other avenues of my life.

TABLE OF CONTENTS

TABLE OF CONTENTS
(Continued)

LIST OF TABLES

LIST OF FIGURES

LIST OF FIGURES
(Continued)

Figure **Page**

CHAPTER 1

INTRODUCTION

1.1 Oil Spills

Marine pollution due to significant crude oil releases pose substantial threats to ecosystems of important environmental and socio-economic values (McGenity, 2014). Chemical dispersants have been widely applied following the blowout of Deepwater Horizon (DWH) rig releasing an estimated 636 million liters of Macondo crude oil into the Gulf of Mexico over the span of 3 months (Camilli et al., 2012; McGenity, 2014). The goal of dispersants is to break the oil into small droplets, which would cause them to dilute (spread) into the water column. Traditionally, the main goal was to prevent the oil slick on the water surface from reaching the shorelines where it could cause more damage, thus becoming more expensive to remove. An added advantage for using dispersants is that the smaller the droplet is, then the larger the specific surface area (surface area divided by the volume of the droplet) becomes. The increase in specific area would increase dissolution in the water column, but more importantly, the biodegradation of oil, which is the degradation of oil by the aid of microorganisms.

Dispersants generally create smaller oil droplets, which increases the oil-water interfacial area per unit mass (or unit volume) of oil. This in turn makes the oil more available for dissolution and biodegradation (Geng et al., 2014; Torlapati & Boufadel, 2014), being that both processes depend directly on the interfacial area. Chemically dispersed oil will have a greater biodegradation rate than physically dispersed oil (A.D.; Venosa & Holder, 2007). However, there are situations where increased dissolution results in high toxicity to micro-organisms, and subsequently inhibition of

biodegradation. Mechanical recovery directly removes oil from the impacted environment, whereas chemical dispersants dilute the oil into small droplets in the water column in order to minimize the impact on the shorelines. The dispersed oil could be removed from the environment through microbial degradation (i.e., biodegradation) (Head, Jones, & Röling, 2006; McGenity, 2014; Prince et al., 2013; Albert D Venosa & Holder, 2013; Yakimov, Timmis, & Golyshin, 2007). The effectiveness of chemical dispersants in mitigating marine oil spills depends on how well the dispersants enhance the dilution of oil.

Oil biodegradation occurs mostly at the oil-water interface since many oil components are not readily soluble in water (Prince et al., 2013). The available surface area to volume ratio of the oil, the biodegradability of hydrocarbons in the dispersed droplets, and the availability of microorganisms at the oil-water interface are also important factors in determining the effects of chemical dispersants on oil biodegradation. The dispersion of oil in seawater depends on the physical properties of oil, namely oil viscosity and interfacial tension with water (Zhao, Boufadel, et al., 2014; Zhao, Torlapati, et al., 2014), on the mixing energy (Kaku, Boufadel, & Venosa, 2006), and on the formulation of the dispersant, in particular the hydrophilic-lipophilic-balance, HLB (Mukherjee & Wrenn, 2013).

1.2 Biodegradation

Rapid and efficient methods of biodegradation are important for the breakdown of oil and hydrocarbons in general that are hazardous to the environment. Biodegradation can occur in either aerobic or anaerobic environments. The presence of oxygen (i.e., aerobic conditions) leads to the fastest biodegradation rates. However, there could be anaerobic

conditions at the sites of spills. For anaerobic conditions, there are different types of terminal electron acceptors (TEAs) that can be used, such as nitrate, sulfate, or ferric iron. Nitrate is a more favorable electron acceptor than sulfate for anaerobic BTEX (benzene, toluene, ethylbenzene and xylene) biodegradation since a greater amount of energy will be released when nitrate is used resulting in faster biodegradation rates than sulfate reduction. According to the laws of thermodynamics, chemical reactions that release the most amount of energy are favored and will thus occur first (Blondina et al., 1999; Dou, Liu, Hu, & Deng, 2008). Nitrate is an effective TEA, but high dosages of nitrate formed from bioremediation can be hazardous in the soil and groundwater where they are left behind. Sulfate is abundant in nature and is found in almost all natural water, so it is often used as a TEA. Sulfate reduction is one of the most efficient anaerobic pathways for degrading petroleum hydrocarbons when looking at it solely based on the stoichiometry of the chemical reaction during biodegradation (Roychoudhury & McCormick, 2006).

The chemical reaction for the aerobic biodegradation of hydrocarbons generally results in carbon dioxide and water. The salinity of the water will affect biodegradation conditions which has previously been reported while experimentally investigating the effect that salinity has on petroleum biodegradation (Mille, Almallah, Bianchi, van Wambeke, & Bertrand, 1991). The amount of oil that will be biodegraded increases with salinity until reaching that of seawater (0.4 mol/L of NaCl). As salinity increases past the level of seawater, the rate of biodegradation decreases. It was also observed that saturated hydrocarbons degrade faster than aromatic and polar compounds (Garrett, Pickering, Haith, & Prince, 1998). Originally, it was assumed that the lack of biodegradation in petroleum-contained aquifers under freshwater conditions was due to the lack of salinity

in the water (Weiner & Lovley, 1998). However, once sulfate-reducing microorganisms were introduced to the system, there was hydrocarbon biodegradation. This was a situation where a lack of indigenous bacteria in that particular region was limiting biodegradation. Therefore, the presence of bacteria is crucial for the biodegradation process.

In addition, oil biodegradation depends also on the availability of oxygen and/or nutrients, including nitrogen and phosphorus (M.C Boufadel et al., 1999; Michel C Boufadel, Sharifi, Van Aken, Wrenn, & Lee, 2010; Bragg, Prince, Harner, & Atlas, 1994; Sharifi, Van Aken, & Boufadel, 2011). Previous studies reported a large range of NO_3-N (~ 2-10 mg/L) concentrations that can support a maximum oil biodegradation rate. In one study, it was concluded that a concentration of about 1-2 mg nitrogen/L could support near optimal biodegradation activity (A. Venosa et al., 1996). Boufadel et al. (1999) demonstrated that a concentration of 2.5 mg NO_3-N/L was sufficient to engender the maximum rate of heptadecane biodegradation. Du et al. found that concentrations close to 10 mg-N/L were required when dealing with oil and not just studying one particular alkane (Du et al., 1999). Phosphorus is also required to support microbial activity and subsequent oil biodegradation and a ratio of N:P of about 10:1 on a mass basis is generally recommended (Ronald M Atlas & Bartha, 1973; Oh, Sim, & Kim, 2003; V. H. Smith, Graham, & Cleland, 1998; Zahed, Aziz, Isa, Mohajeri, & Mohajeri, 2010).

In this study, we investigated the aerobic degradation of physically dispersed and chemically dispersed Alaska North Slope (ANS) crude oil under aerobic laboratory conditions. The experiment aimed at (1) comparing the effect of the droplet size

distributions of dispersed oil on biodegradation rates, and (2) evaluating the impact of nutrient amendment on the biodegradation rates of dispersed oil.

CHAPTER 2

METHODS

2.1 Water Sample Collection and Filtration

Samples were collected from the Atlantic Ocean at the beach in Atlantic City, NJ (39.353197, -74.435085). Certified-clean amber-glass jugs were individually held 10-15 cm below the water surface, filled by simply removing the cap, and closed before returning to the surface. The jugs were kept on ice in coolers that were transported to the laboratory at NJIT (Newark, NJ) within 4 hours. The samples were then placed into the fridges and kept at 4^{o} Celsius before using them for the experiment. The samples were filtered through a 10μm Whatman paper filter using a filtering flask and a Buchner funnel in order to remove flagellates, ciliates, and other bacterial grazers. These may increase the variability among the triplicate microcosms. It is often stated that this might have the consequences of overestimating oil biodegradation, as the absence of grazers allows the hydrocarbon degrading bacteria to thrive. However, the addition of oil has been shown to kill the grazers more than it affects bacteria.

2.2 Oil Biodegradation in Respirometric-microcosms

Alaskan North Slope (ANS) crude was obtained from the Bedford Institute of Oceanography located in Dartmouth, Nova Scotia. Samples was mixed in a 250-mL screw-cap trypsinizing flask (an Erlenmeyer flask with baffles) that has been modified with the placement of a glass stopcock near its bottom so that a subsurface water sample can be removed without disturbing the surface oil layer (see Figure 2.1). For each sample, an amount of 0.75 mL oil and 0.075 mL dispersant (Corexit 9500) was added to 150 mL

seawater. This was performed by measuring the mass of the quantity of oil in a glass syringe and then slowly dripping the oil onto the surface of the seawater in the baffle flask. The empty syringe was weighed to find the actual mass of oil added. For the chemical dispersion, 0.75 mL of the dispersant was gently added to the center of the oil surface on top of the water (dispersant to oil ratio (DOR) - 1:10 (v/v)). Initial mixing in baffle flasks was performed for an initial time period of one hour at mixing speeds of 250 and 125 RPM. The water was chemically enhanced with 100 mg NO3-N/L and 10 mg PO4-P/L to form a high nutrient condition for certain samples that were mixed at each of the mixing speeds. Additionally, samples were shaken at the higher mixing speeds both with and without the presence of 0.5% w/v of sodium azide to act as a control in which microbial activities were limited. Experimental parameters are depicted in table 2.1.

Figure 2.1 Photograph of a baffled trypsinizing flask.
Source: Venosa et al., 2013

Table 2.1 Experimental Parameters

Experimental Condition	Experiment Code	Speed (RPM)	Nitrate conc (mg/L)	Phosphate conc (mg/L)	Sodium azide conc (w/v %)
High speed, high nutrient	HSHN	250	100	10	0
Low speed, high nutrient	LSHN	125	100	10	0
Control	C	250	0	0	0.5
High speed, low nutrient	HSLN	250	0	0	0

A number of significant parameters (oil concentration, biomass production, O2 consumption, CO2 production and nutrient consumption) of ANS crude biodegradation will be evaluated using sealed respirometric-microcosms (Fisher, 2005). After the initial mixing time period of 1 hour, a volume of 100 mL of the subsurface sample of the oil-water mixture was added to each sealed 250 mL microcosm (see Figure 2.2). Thus, four conditions were examined in total (high speed, high nutrient; low speed, high nutrient; high speed, low nutrient; and the control with sodium azide) at four different time points (0, 14, 28, 42 days). Triplicates of each case resulted in the initial amount of 48 respirometric flasks being mixed. The entire experiment was conducted for the duration of 42 days. The microcosms were continuously agitated by the orbital shakers and kept in the incubators at a constant temperature (15 ± 0.5 °C). Three independent replicate microcosms were sacrificed each time sampling was performed.

The microcosms were constructed with a CO_2 trap filled with a trapping solution (sodium hydroxide) and a sample port located in the cap of the trap tubes for replacing the trapping solution. The production of carbon dioxide was periodically measured by the

titration of CO_2 trapping solution with phenolphthalein to find the endpoint using sulfuric acid to achieve a pH of 8.3. Oxygen demand was measured by attaching a 60-ml oxygen-filled ground-glass syringe to the sidearm of the microcosm. The pressure of the syringe barrel was then equalized with the microcosm headspace gas pressure. The amount of oxygen that entered the microcosm was recorded. Oxygen demand was measured at an interval of two days initially and then decreased towards the end of the experiment (42 days).

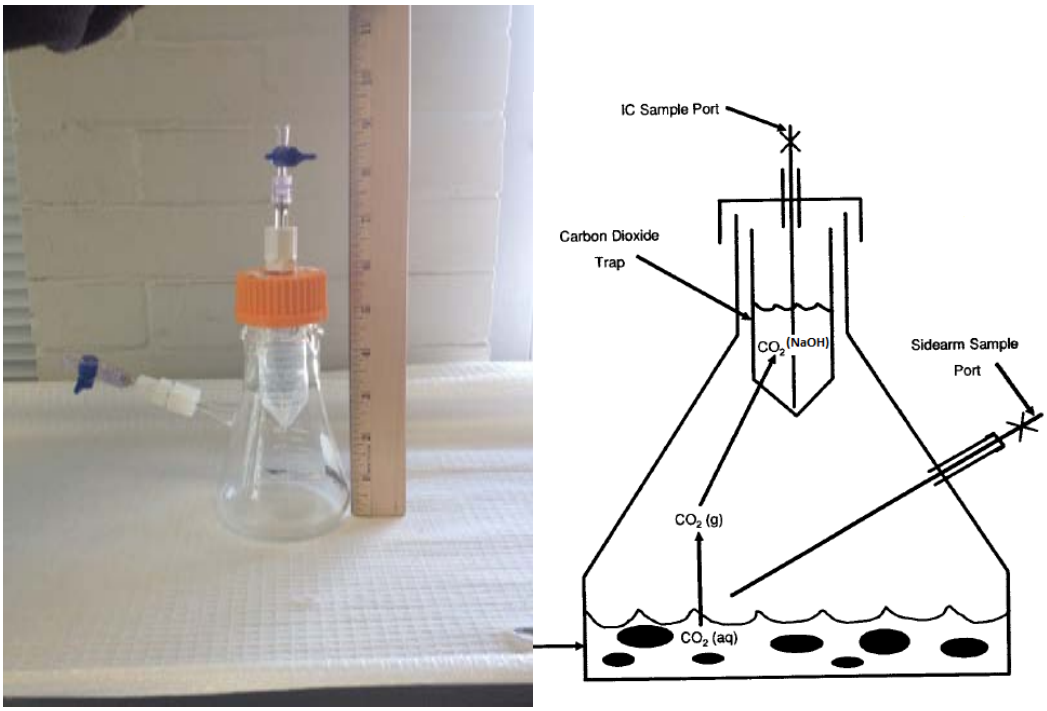

Figure 2.1 Swirling flask with a sidearm for oxygen replenishment and measurement, and the carbon dioxide trap.

Source: Venosa et al., 2013

2.3 Oil Standards Procedure

Oil standards were made to allow for the formation of a calibration curve. For generating a 6-point calibration curve, specific volumes of oil were added (20, 50, 100, 150, 200, and 300 µL) to 30 mL seawater in a 125 mL separatory funnel. Dispersant (Corexit 9500)

was added to each sample in the amount of 1:10 DOR (v/v) in the same manner as when the samples were prepared. Liquid/liquid extractions (explained in detail in section 2.4) of each sample was then performed three times by using 5 mL of dichloromethane (DCM) for each extraction and adjusting the final extract to 44 mL. The final extract was transferred to 44 mL crimp style glass vials with aluminum/Teflon seals and stored at 5 ^{o}C until the time of analysis (never exceeding two days). Absorbance values were measured for each of the concentration values with a spectrophotometer (Cole Parmer 4802 UV double beam).

2.4 Determination of Oil Concentration

The total petroleum hydrocarbon (TPH) concentration was measured at time zero (after mixing oil with water) and at intervals of 2 weeks (14 days) until the end of the experiment (42 days). The TPH values were obtained by measuring absorbance with the spectrophotometer after liquid-liquid extraction with dichloromethane (DCM). The extraction procedure involves putting 30 mL of the dispersed oil-water mixture into a 125 mL separatory funnel and then adding 5 mL DCM and shaking vigorously for about 2 minutes. The DCM-oil phase and water phase was then given approximately 5 minutes to separate from each other. The bottom layer, consisting of DCM-oil was then drained using the stopcock into a clean beaker (EPA Method 3510C (EPA, 1996)). This was performed at least 3 times until the DCM phase was colorless, indicating that there was no more oil in the separatory funnel. To ensure all of the water was removed from the sample, a funnel was lined with glass wool and a layer of anhydrous sodium sulfate was placed on top to cover the glass wool. The DCM-oil layer was then slowly poured through the funnel. DCM was used to occasionally rinse all of the oil off of the sides of

the beaker that held the extract and also used to flush any oil that remained attached to the glass wool or inside the funnel. The extract was adjusted to a final volume of 44 mL and then transferred to a 44 mL crimp style glass vial with an aluminum/Teflon seal. The vials were stored at 5 ^{o}C until the time of analysis, and the holding time never exceeded 2 days. The absorbance values of the samples were measured at wavelengths of 340, 370 and 400 nm by using the spectrophotometer. The absorbance was measured against the wavelength and the area under the curve was calculated by using the following equation:

$$Area = \frac{(Abs_{340} + Abs_{370}) \times 30}{2} + \frac{(Abs_{370} + Abs_{400}) \times 30}{2} \quad (2.1)$$

The symbols Abs_{340}, Abs_{370}, Abs_{400} stand for the absorbance values at wavelengths of 340, 370 and 400 nm, respectively. The area calculated was then used for calculating the total amount of oil dispersed:

$$Total\ Oil\ dispersed = \frac{Area}{Calibration\ Curve\ slope}\ X\ V_{DCM} X \frac{V_{tw}}{V_{ew}} \quad (2.2)$$

From equation 2.2, V_{DCM} represents the volume of DCM, V_{tw} is total volume of sea-water in the flask, and V_{ew} is total volume of sea-water extracted.

2.5 Oil Droplet Size Distribution

The oil droplet size distribution was measured with the Laser In Situ Scattering and Transmissometry (LISST) 100X (Sequoia Scientific Inc). The lens and mixing chamber was cleaned with alcohol wipes and then the chamber was flushed with deionized water multiple times. Roughly 125 mL deionized water was poured inside the LISST chamber and the background measurement (automatically collected for 20 samples) was recorded and saved as long as no error messages were present. The water was drained from the chamber. One milliliter of sample was extracted with a 100-1000 µL Fisherbrand Finnpipette® II Adjustable Pipette and a 100-1250µL Fisher Scientific tip and then was diluted with 120 mL deionized water. The dilute suspension was carefully poured into the LISST chamber. The Real - Time Session of the file menu was opened and the appropriate background file was also opened to process the data. An output PSD file was made and two plots on the left and right hand side was displayed. The figure on the left hand side showed the volume concentration in each of the 32 log spaced size classes. The right hand side plot showed the cumulative concentration. Interfacial area was calculated once the oil droplet distributions were measured. It was found by dividing the volume fraction by the volume of the oil droplet and then multiplying that by the area of the droplet.

2.6 Biomass Estimation

In addition to studying the oil, oxygen, and CO_2 in the microcosms, the most probable number (MPN) method was used to estimate biomass production including alkane degraders, PAH degraders, and heterotrophic bacteria. The MPN assay was conducted using 96-well tests. Alkane and PAH degraders was incubated in Bushnell-Hass Broth

(BHB) (Difco Laboratories, Sparks, MD) medium (0.2 g/L of $MgSO_4$; 0.02 g/L of $CaCl_2$; 1.0 g/L KH_2PO_4; 1.0 g/L of $(NH_4)_2HPO_4$; 1.0 g/L of KNO_3; 0.05 g/L of $FeCl_3$). A volume of 5 μL of filter-sterilized hexadecane was added as a carbon source to each well of the alkane-degrader plates. Prior to the addition of BHB, PAH-degrader plates was coated with a solution of phenanthrene (10g/L), fluorene (1g/L), and dibenzothiophene (1g/L) in pentane. Additionally, yeast extract with a concentration of 0.2 g/L was added to PAH medium to meet nutrient requirements for PAH degraders. Heterotrophic bacteria was incubated in PTYG medium containing 0.25 g/L of peptone, 0.25 g/L of trypticase soy broth, 0.5 g/L of yeast extract, 0.5 g/L of glucose, 0.6 g/L of $MgSO_4 \cdot 7H_2O$, and 0.07 g/L of $CaCl_2 \cdot 2H_2O$.

Samples were collected from the microcosms every two weeks at day 0 (after 1 hour of mixing oil and dispersant with water), 14, 28 and 42. After the plates were inoculated with the samples, they were incubated in the dark at room temperature (~20 ºC) for two weeks for alkane and heterotrophic plates, and 3 weeks for PAH plates. After the incubation, positive wells indicate growth of bacteria. Positive PAH plates (or wells) turn yellow, brown or green from accumulation of the partial oxidation products of the aromatic substrates (Wrenn & Venosa, 1996). Positive plates for alkane degraders and heterotrophic bacteria turn red as INT, which is a pale yellow solution, was added to the plates. INT will reduce to an insoluble bright red formazan dye by aerobic respiratory chains while negative wells remain colorless or pale yellow (Wrenn & Venosa, 1996). The concentration (number of cells/L) of each bacterial group was estimated from the number of positive wells in each row of dilutions showing evidence of microbial growth.

Biomass concentrations as mg/L were calculated from the MPN numbers assuming a cell dry weight of 2.8×10^{-10} mg (Rittman & McCarty, 2001).

2.7 Nutrient Concentration

Nutrient concentrations in the filtered water were analyzed using a spectrophotometer (Cole Parmer 4802 UV double beam). Background nutrient concentrations of the samples were taken at time zero. Nitrate and phosphate concentrations were determined based on reading absorbance values and comparing them to calibration curves of stock solutions. Nitrogen and phosphorous consumption were calculated based on biomass formula ($C_5H_7O_2NP_{0.1}$) (Rittman & McCarty, 2001). Nutrient calculations are based on stoichiometric relationships between the nutrients and the assumed biomass formula of $C_5H_7O_2NP_{0.1}$. According to the calculation, per 1 mg of dry biomass formed, 0.121 mg of nitrogen and 0.027 mg of phosphorous are consumed.

2.8 Oxygen Consumption and Carbon Dioxide Production Measurements

The mass of oxygen consumed by microbial metabolism over time was calculated by using the recorded values of the volume of oxygen added to the microcosm via the glass-ground syringe. The following equation was used:

$$M_{O_2}(t) = \frac{P \times V_{O_2} \times MW_{O_2}}{R \times T} \tag{2.3}$$

In the previous equation, P is atmospheric pressure of 1 atm, MW_{O2} is molecular weight of oxygen of 32 g/mole, R is the ideal gas constant of 82.054 ml-atm/mole-K, and T is incubation temperature in K.

The mass of carbon dioxide produced for each microcosm was determined by performing a titration of the CO_2 trapping solution. A 0.04 M sodium hydroxide solution for trapping carbon dioxide in microcosms was prepared. Approximately 20 ml was inserted into the top port of the microcosm with a plastic syringe. At each time point, before opening each microcosm, the trapping solution was pulled out with a syringe and the mass was measured. This was then poured into a 125-ml Erlenmeyer flask and mixed with a magnetic stirrer. About 5 drops of phenolphthalein indicator was added to the solution, which turned the solution pink. A self-zeroing buret was filled with 0.1-N sulfuric acid and it was made sure that no air bubbles remained in the buret. Titration was performed by allowing the sulfuric acid to gently drip into the solution. Titration was stopped as soon as the color indicator completely disappeared and the solution turned clear. The volume of sulfuric acid added was recorded.

A sodium carbonate standard solution was prepared and the actual concentration of it was calculated. Then, that standard solution was used to calculate the actual concentration of sulfuric acid titrant before the concentration of the sodium hydroxide trapping solution was found with the following equation:

$$\left[NaOH\right]_{fresh} = 2\left[H_2SO_4\right]\frac{V_{H_2SO_4}}{V_{NaOH}} \tag{2.4}$$

In the previous equation, $[NaOH]_{fresh}$ is the molar concentration of sodium hydroxide solution (mole/liter), $[H_2SO_4]$ is the molar concentration of sulfuric acid (mole/liter), V_{H2SO4} is equal to the volume of sulfuric acid needed to reach the endpoint (ml), and V_{NaOH} indicates the volume of sodium hydroxide solution that was titrated (ml).

In order to determine the concentration of carbon dioxide in the trapping solution for each sample, the following equation was used:

$$[CO_2]_{trap} = [NaOH]_{fresh} - V_{H_2SO_4} \times 2[H_2SO_4] \quad (2.5)$$

The variable, $[CO_2]_{trap}$, is equal to the concentration of carbon dioxide absorbed by the trapping solution (mole/liter).

The mass of carbon dioxide carbon ($M_{CO2\text{-}C}$, g C) that was produced in the microcosm between the time that the fresh trapping solution was added (t_i) and the time at which the sample was analyzed (t_{i+1}) was determined with the following equation.

$$M_{CO2-C} = V_{NaOH} \times [CO_2]_{trap} \times AW_C \quad (2.6)$$

The symbol, AW_C, refers to the atomic weight of carbon (12.01 g/mole).

CHAPTER 3

RESULTS

3.1 Oil Droplet Distribution

The various experimental conditions led to different oil droplet distributions at the initial time of zero. The median oil droplet diameter size for the high speed, high nutrient (HSHN) condition was the smallest initial value of 3.00 microns. All of the high speed cases were mixed at 250 RPM, including the control (C) case and the high speed, low nutrient (HSLN) case, which had initial median oil droplet diameters of 3.48 and 3.15 microns, respectively. Switching to a mixing speed of 125 RPM for the low speed, high nutrient (LSHN) case yields a higher median diameter of 4.34 microns. The initial oil droplet size distributions, illustrated as both a cumulative volume fraction and a volume fraction versus oil droplet size, can be seen in Figure 3.1 and Figure 3.2, respectively. The volume fraction curve clearly displays the larger oil droplet distribution that results from the lower mixing speed. Both figures show that the HSHN has the smallest oil droplet size distribution after initial mixing for one hour.

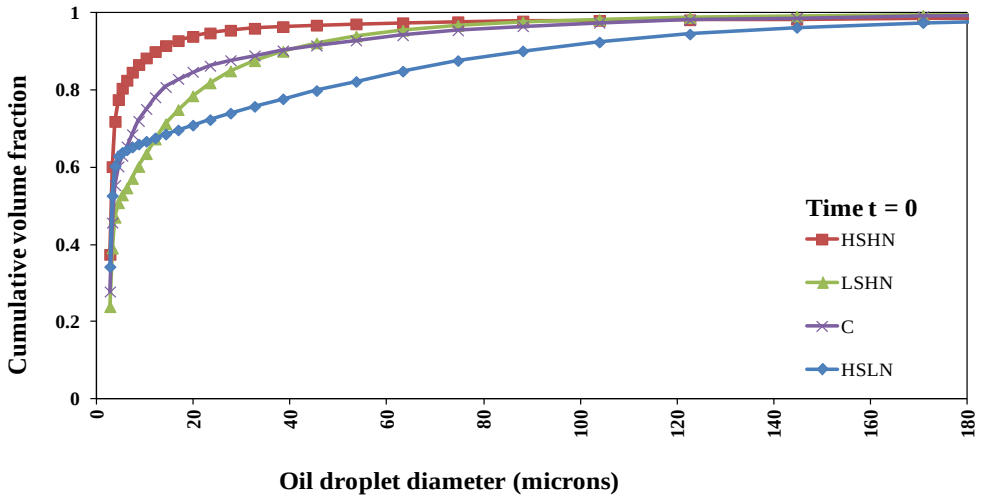

Figure 3.1 Cumulative volume fraction versus oil droplet diameter size at time zero for each of the experimental conditions.

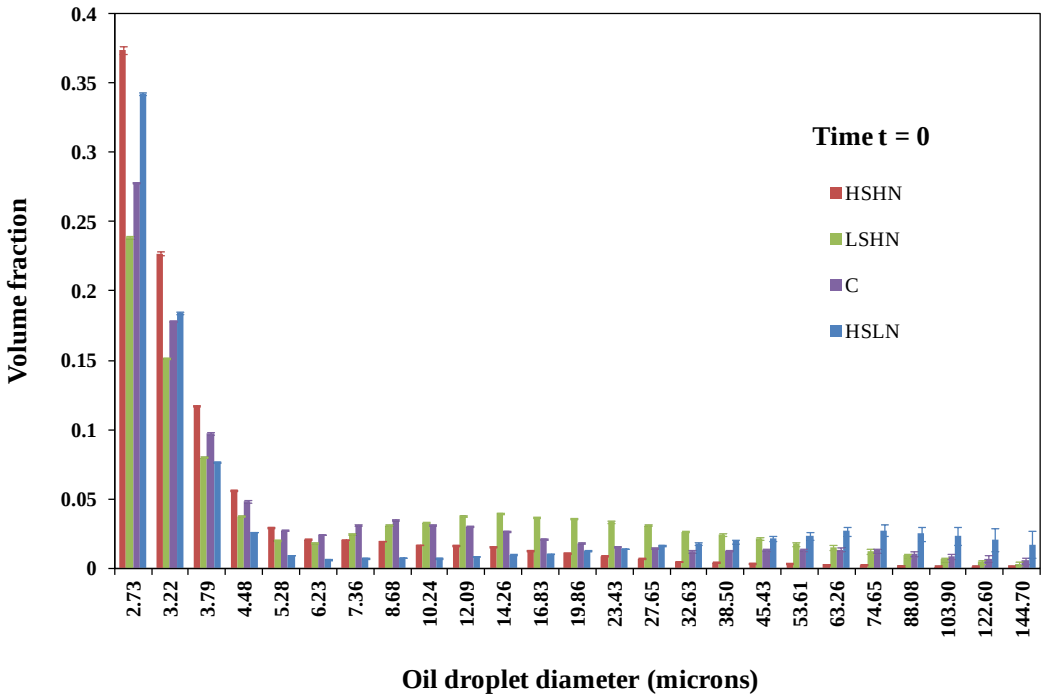

Figure 3.2 Volume fraction versus oil droplet diameter size at time zero for each of the experimental conditions.

Table 3.1 depicts the temporal changes for each of the oil droplet distributions. Figure 3.3 shows how the log median oil droplet diameter changes over time for each of the conditions. The high speed, high nutrient (HSHN) case increases to 10.78 microns after a duration of 2 weeks (time t = 1) and then it increases very slightly until it levels off afterwards. This increase in diameter was due to the smaller oil droplets being consumed by the bacteria. The control (C) case and the high speed, low nutrient (HSLN) case both have a median oil droplet size in the range of 3-5 microns during the entire study. Over time, the LSHN case drastically increases to a median diameter of 233 microns after 42 days. The initial larger oil droplet sizes end up coalescing over time.

Table 3.1 Median Oil Droplet Diameter Size

Time (days)	**Time interval (t)**	**Median diameter size (microns)**			
		HSHN	**LSHN**	**C**	**HSLN**
0	0	3.00	4.34	3.48	3.15
14	1	10.78	2.78	3.24	3.74
28	2	16.38	19.51	3.22	2.78
42	3	14.23	233.46	3.36	4.28

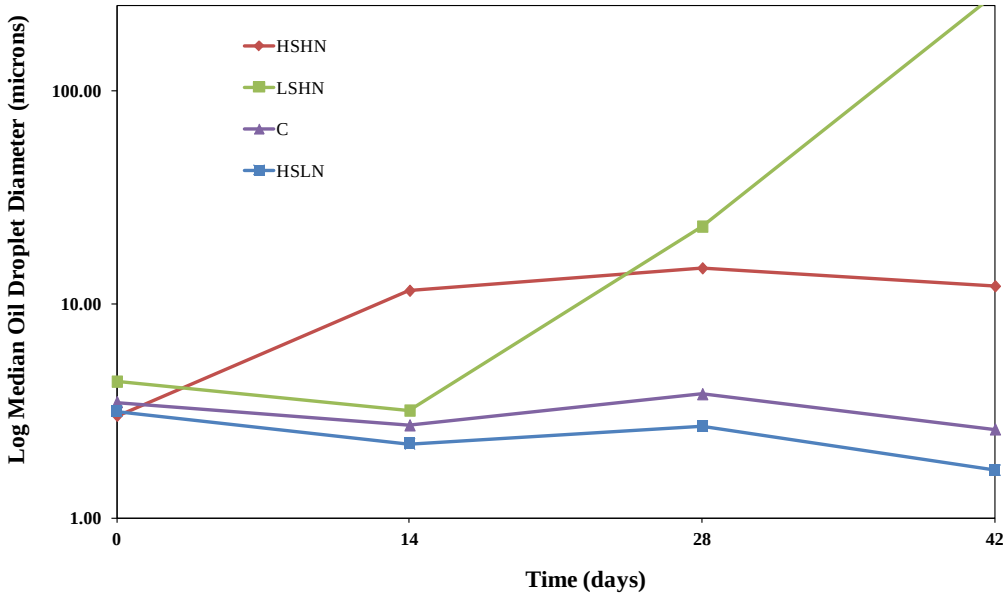

Figure 3.3 Log median oil droplet diameter size versus time for each of the experimental conditions

Figures 3.4 and 3.5 shows the cumulative volume fraction and the volume fraction versus time at time one, respectively. All of the distributions show relatively small diameter sizes. Figures 3.6 and 3.7 shows the cumulative volume fraction and the volume fraction versus time at time two, respectively. The LSHN and C cases show a spike in the larger diameters in the volume fraction histogram, which is indicative of a droplet distribution that has both small and large droplet diameters.

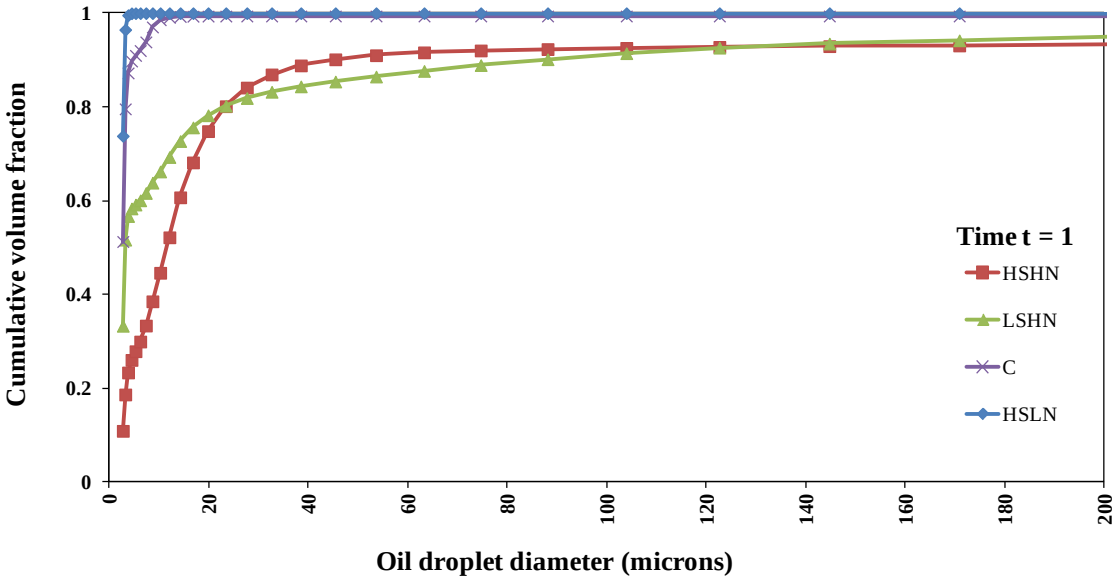

Figure 3.4 Cumulative volume fraction versus oil droplet diameter size at time one for each of the experimental conditions.

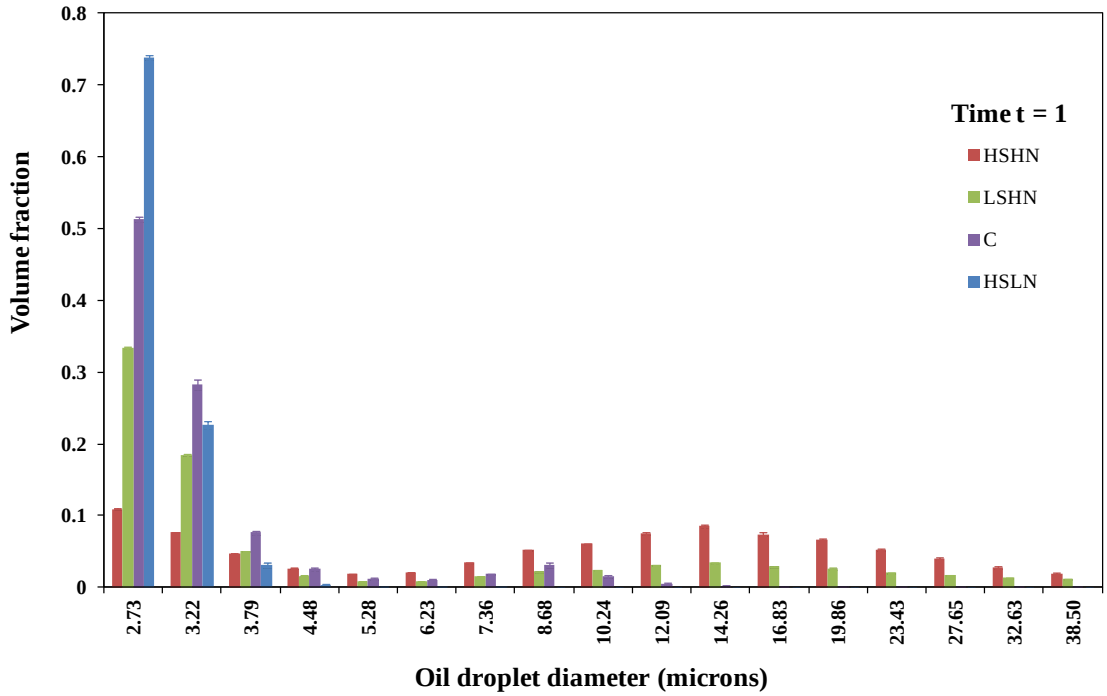

Figure 3.5 Volume fraction versus oil droplet diameter size at time one for each of the experimental conditions.

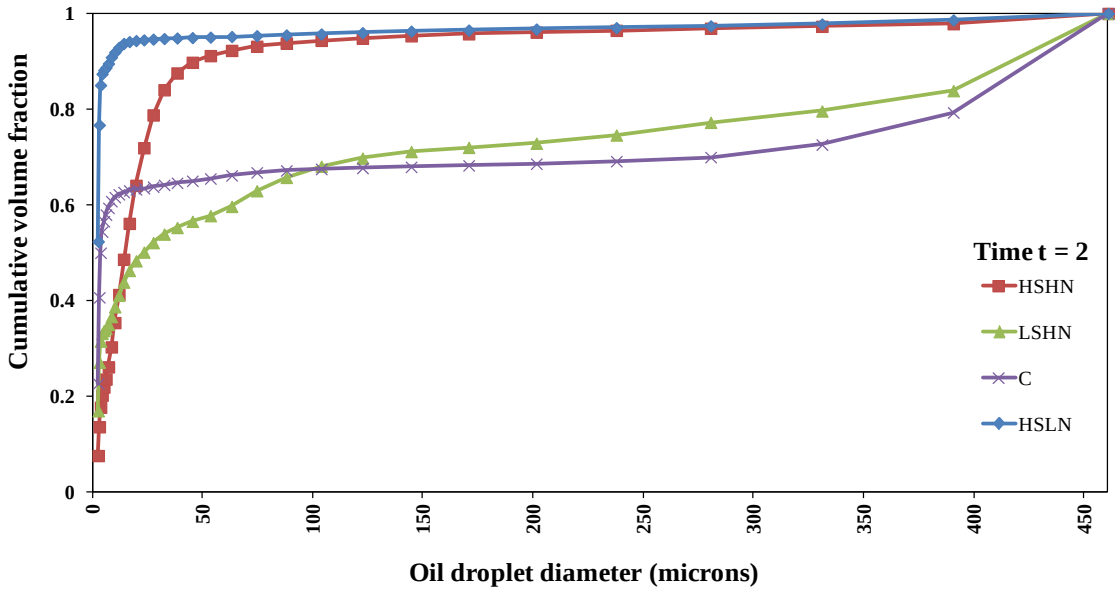

Figure 3.6 Cumulative volume fraction versus oil droplet diameter size at time two for each of the experimental conditions.

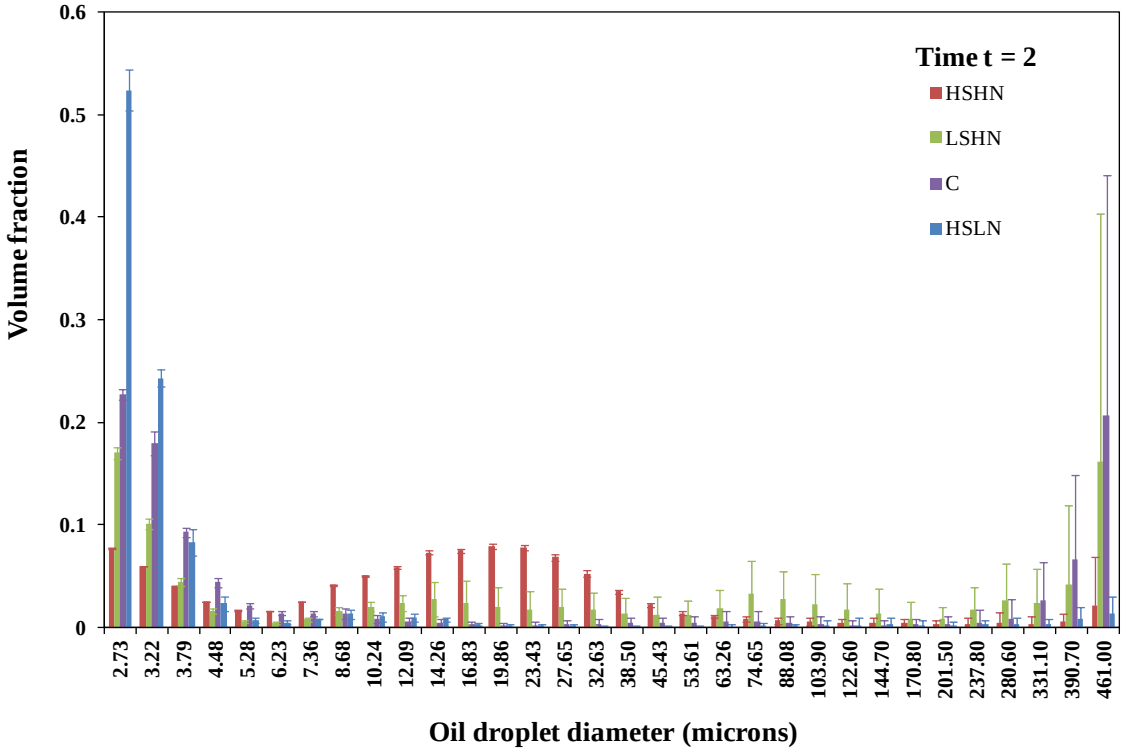

Figure 3.7 Volume fraction versus oil droplet diameter size at time two for each of the experimental conditions.

The cumulative volume fraction versus time and the volume fraction versus time at time three can be seen in Figures 3.8 and 3.9, respectively. HSHN has a small droplet distribution with a median particle size diameter of 14.23 microns. LSHN shows many of the larger droplet diameter sizes in both figures. HSLN has a spike in volume fraction at the low end of the diameter sizes and then a smaller peak at the larger end.

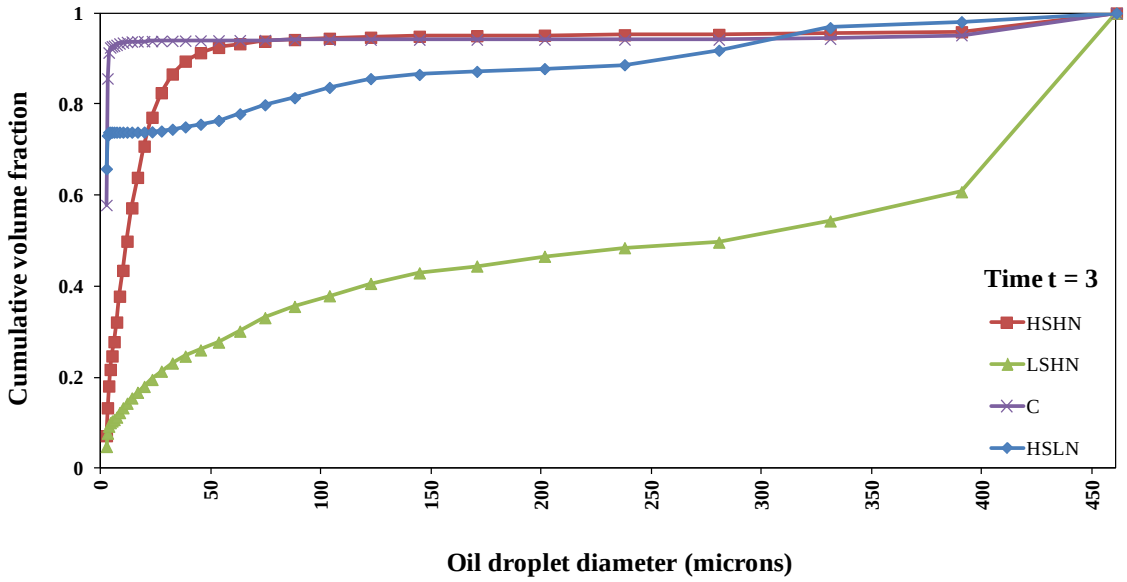

Figure 3.8 Cumulative volume fraction versus oil droplet diameter size at time three for each of the experimental conditions.

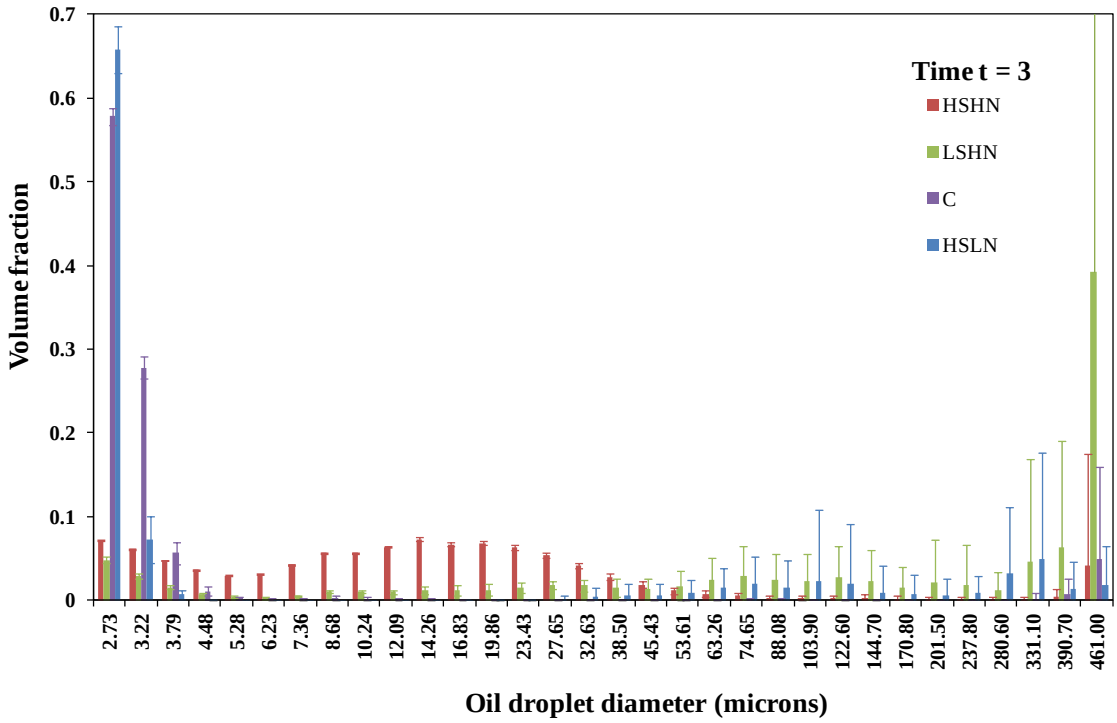

Figure 3.9 Volume fraction versus oil droplet diameter size at time three for each of the experimental conditions.

3.2 Oil-water Interfacial Area

The oil-water interfacial specific area was calculated by dividing the volume fraction of the oil droplets by the volume of the oil droplet and then multiplying that number by the area of the oil droplet. This was performed for each experimental condition over time and the values are presented in Table 3.2. Figure 3.10 shows the interfacial specific area versus oil droplet diameter size at time zero. The high speed, high nutrient (HSHN) case has the largest interfacial specific area of 1.63 $\pm$ 0.20 microns^{-1} after the initial mixing period at time zero. The oil droplets in this case have the largest surface area at the beginning of the study.

Table 3.2 Interfacial Specific Area

Time (days)	Time Interval t	Experiment Condition	IFA average (1/microns)	IFA std dev (1/microns)
0	0	HSHN	1.63	0.20
		LSHN	1.18	0.12
		C	1.34	0.25
		HSLN	1.33	0.31
14	1	HSHN	0.79	0.24
		LSHN	1.31	0.63
		C	1.88	0.22
		HSLN	2.10	0.08
28	2	HSHN	0.66	0.11
		LSHN	0.77	0.09
		C	1.12	0.26
		HSLN	1.82	0.08
42	3	HSHN	0.72	0.09
		LSHN	0.27	0.28
		C	1.91	0.13
		HSLN	1.61	0.16

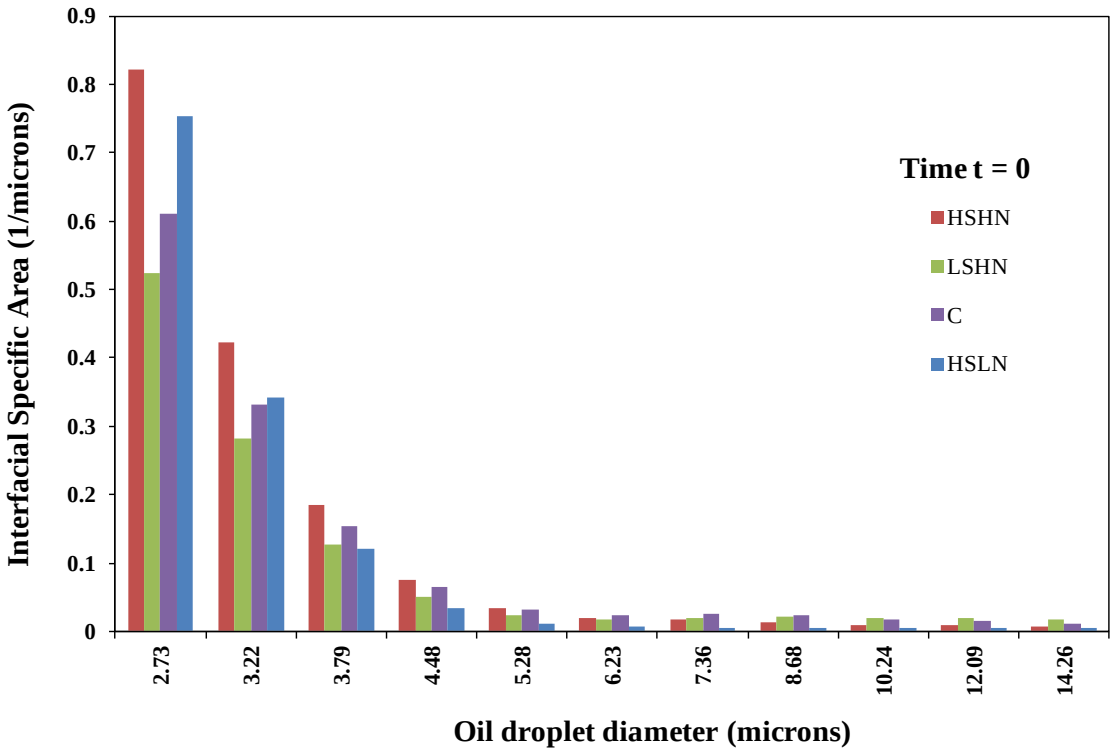

Figure 3.10 Interfacial specific area versus oil droplet diameter size at time zero for each of the experimental conditions.

Figures 3.11, 3.12, and 3.13 show the interfacial specific area versus oil droplet diameter size at times one, two, and three, respectively. Due to the larger surface area, the smaller HSHN droplets gets eaten by the microbes, so the interfacial specific area decreases down to 0.79 $\pm$ 0.24 microns^{-1} at time 1 as the smaller droplets disappear.

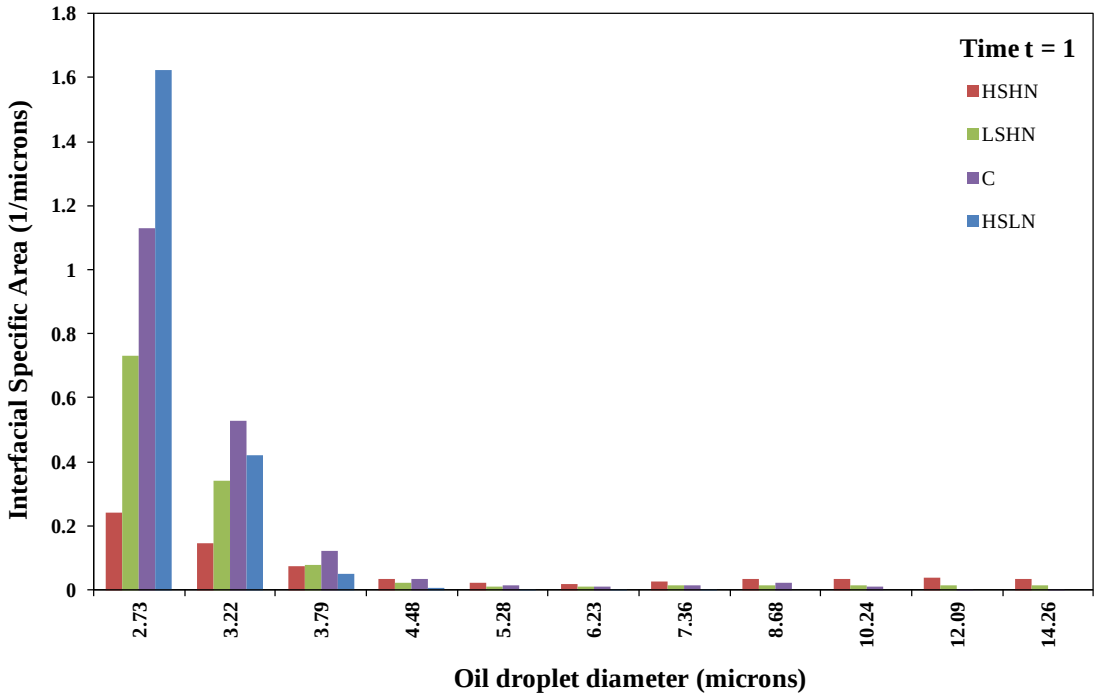

Figure 3.11 Interfacial specific area versus oil droplet diameter size at time one for each of the experimental conditions.

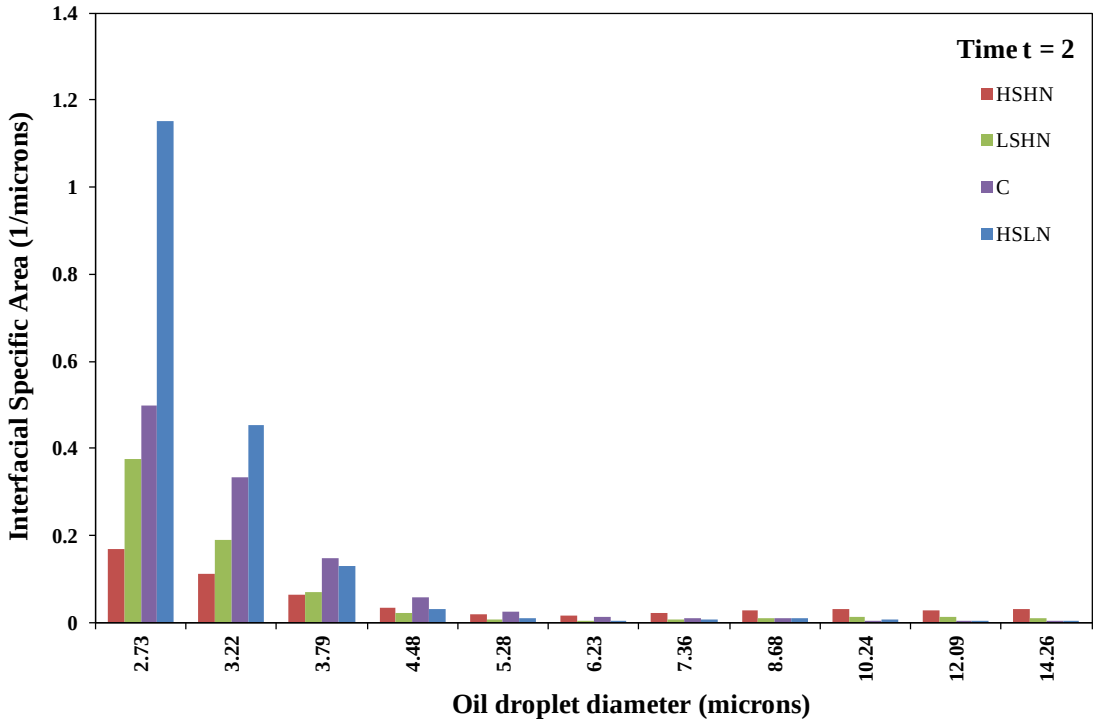

Figure 3.12 Interfacial specific area versus oil droplet diameter size at time two for each of the experimental conditions.

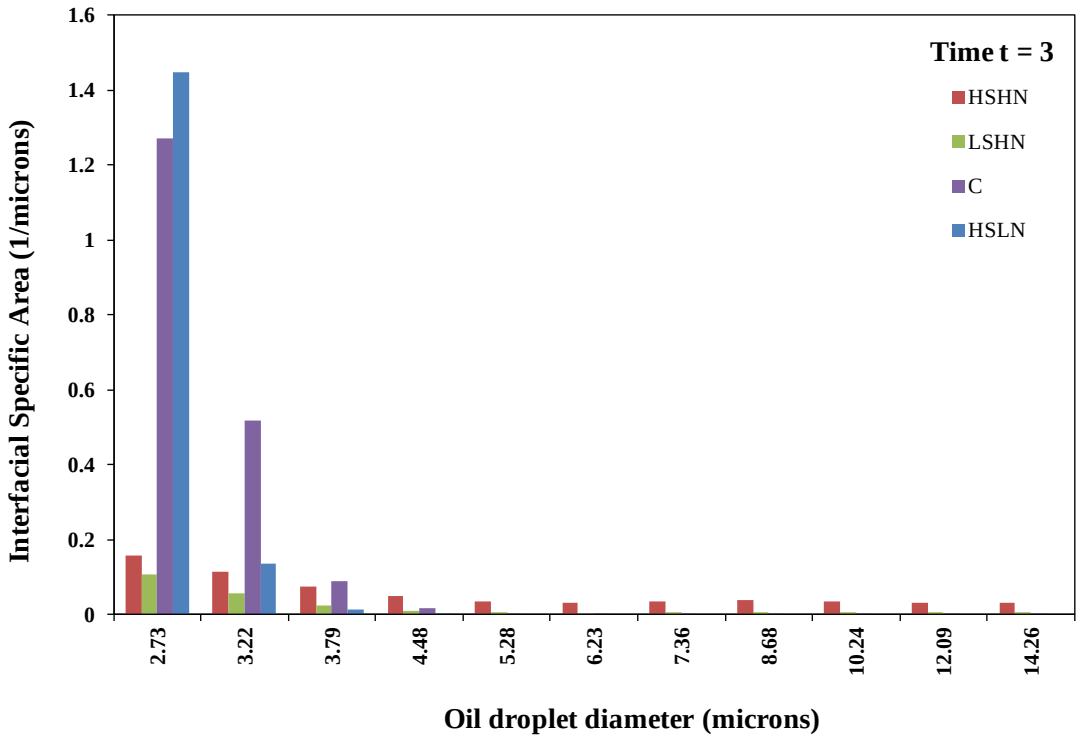

Figure 3.13 Interfacial specific area versus oil droplet diameter size at time three for each of the experimental conditions.

3.3 Initial and Temporal Changes in Oil Concentration

The oil concentration was measured at the start of this experiment and at each time point for each of the experimental cases. The oil values are reported as total petroleum hydrocarbon (TPH) in Table 3.3. The plot of TPH versus time can be found in Figure 3.14. Time zero indicates various initial concentrations of oil for each experimental condition. The same volume of oil was added to each of the baffle flasks prior to mixing and the masses were recorded. However, for the case of low speed, high nutrient (LSHN), the lower mixing rate failed to mix the oil into the water column to the same extent as the other cases. This resulted in a measurement of only 0.189 grams of oil; as opposed to the full quantity that remained as an oil slick inside the baffle flask (only oil dissolved into the water column was used for analysis by sampling through the stopcock). The initial

values for the other trials ranged from 0.622 grams of oil (high speed, high nutrient) to 0.428 grams of oil (control). In literature, oil has been observed to adhere to the walls of glassware during mixing stages resulting in initial TPH values being measured lower than actual quantities (Campo, Venosa, & Suidan, 2013). In certain instances even when Corexit 9500 is used, up to 30% of the initial oil can be lost due to oil adhering to the glassware (Bælum et al., 2012).

Table 3.3 Total Petroleum Hydrocarbon (TPH) Values

Time (days)	Time Interval t	Experimental Condition	TPH avg mass (g)	TPH std dev (g)
0	0	HSHN	0.62	0.12
		LSHN	0.19	0.02
		C	0.43	0.09
		HSLN	0.46	0.11
14	1	HSHN	0.26	0.14
		LSHN	0.22	0.09
		C	0.35	0.22
		HSLN	0.08	0.03
28	2	HSHN	0.11	0.11
		LSHN	0.01	0
		C	0.32	0.33
		HSLN	0.04	0.04
42	3	HSHN	0.19	0.17
		LSHN	0.09	0.05
		C	0.23	0.11
		HSLN	0.06	0.02

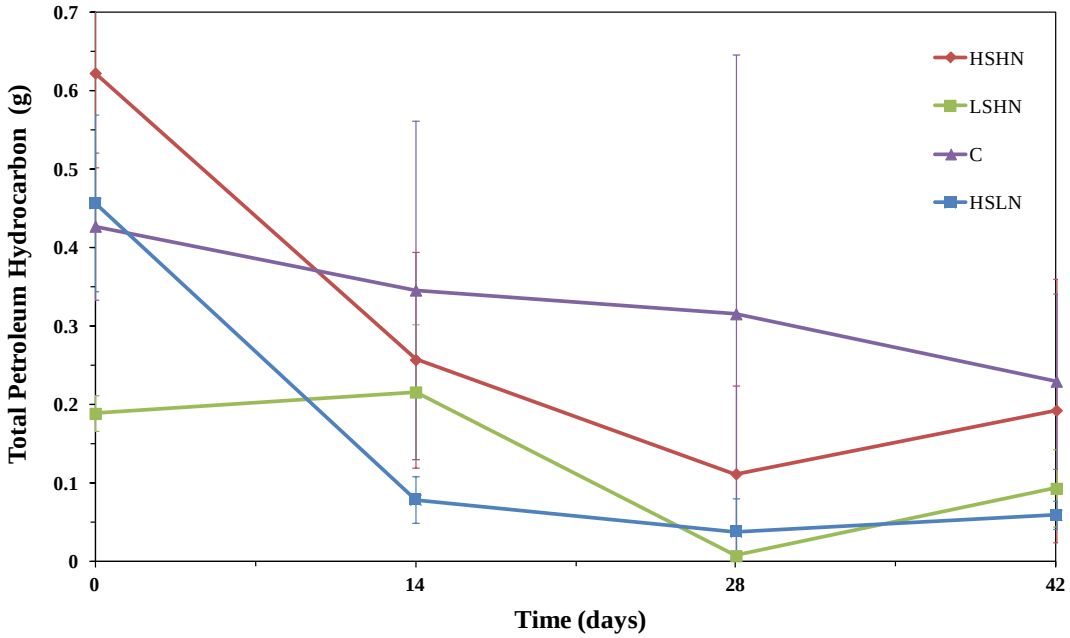

Figure 3.14 Total petroleum hydrocarbon (TPH) versus time for each of the experimental conditions.

TPH versus time for the HSHN case revealed that 82% of the initial oil was biodegraded. This occurs at time 2, which is the peak of biodegradation for this case. The slight uptick in TPH mass at time 3 is still within the error bars. These samples started out with the largest quantity of oil for all of the cases. The LSHN case shows a discrepancy since there is a maximum amount of 96% oil removed from the water column during the study, yet there is a large increase in oil mass from time 2 to time 3 resulting in only 51% of oil removal. The actual value may be somewhere in between those values, but probably closer to 51% since it is impossible for oil to be produced after it has already been degraded. This case started with a TPH that was 3 times less than the mass of oil in the HSHN case since the water was not well mixed into the water column due to the lower initial speed. The HSLN case has an amount of 87% oil removal at time 2, while there is only a slight increase at time 3. This case presents the largest rate of

biodegradation, which indicates that the presence of nutrients is not as important of a factor as mixing speed. Also, it may be due to the fact that there is less initial oil in the water column compared to the HSHN case.

It was concluded that the control case had the least amount of oil mass removal in this study. The amount of oil removed for the control case was 46% of the initial mass. Loss of oil mass for the control can be attributed to the oil droplets adhering to the sides of the microcosm. This was confirmed visually since large amounts of oil were found stuck to the side of the microcosm relative to all of the other cases. It has been noted in literature that oil adheres more to the glassware walls with the presence of sodium azide, which was used in this case as a bacteria killing agent (J. Smith, Dore, Pope, Balba, & Weston, 2007). Therefore, there was actually less than 46% of oil loss by evaporation or physical degradation. The sodium azide was added to kill any bacteria so that there would not be any oil removed via biodegradation.

3.4 Biomass Production

Temporal variations in the microbial production was measured in cells/mL for alkane degraders, PAH degraders, and heterotrophic bacteria. Note that the presence of PAH degraders were observed to be zero for all of the experimental conditions during the course of this six week study, so these plots and values have not been included. The log most probable number (MPN) of the microbial population values for alkane degraders can be found in Table 3.4. Also, the log MPN for alkane degraders was plotted as a function of time for each condition in Figure 3.15. The initial (time t = zero) log MPN for alkane degraders were all low values ranging from 0 to 0.23 cells/mL. The largest bacterial peak in the presence of alkane degraders for each of the cases, occurred between

times 1 and 2 for the HSHN case, when the amount of cells/mL increased from 0.15 to 1.52. The LSHN case showed the second largest bacterial peak of 1.20 cells/mL, which occurred at time 3. The HSLN case had a very low presence of alkane degraders. The highest value that it reached was at time 2, when the log MPN was measured as 0.25 cells/mL. The MPN experiment for the control, C, did not detect the presence of alkane degraders during the course of the entire study.

Table 3.4 Log Most Probable Number (MPN) Values for Alkane Degraders

	Log MPN (cells/mL)			
Time (days)	**HSHN**	**LSHN**	**C**	**HSLN**
0	0.11	0.00	0.00	0.23
14	0.15	0.59	0.00	0.15
28	1.52	0.73	0.00	0.25
42	1.27	1.20	0.00	0.05

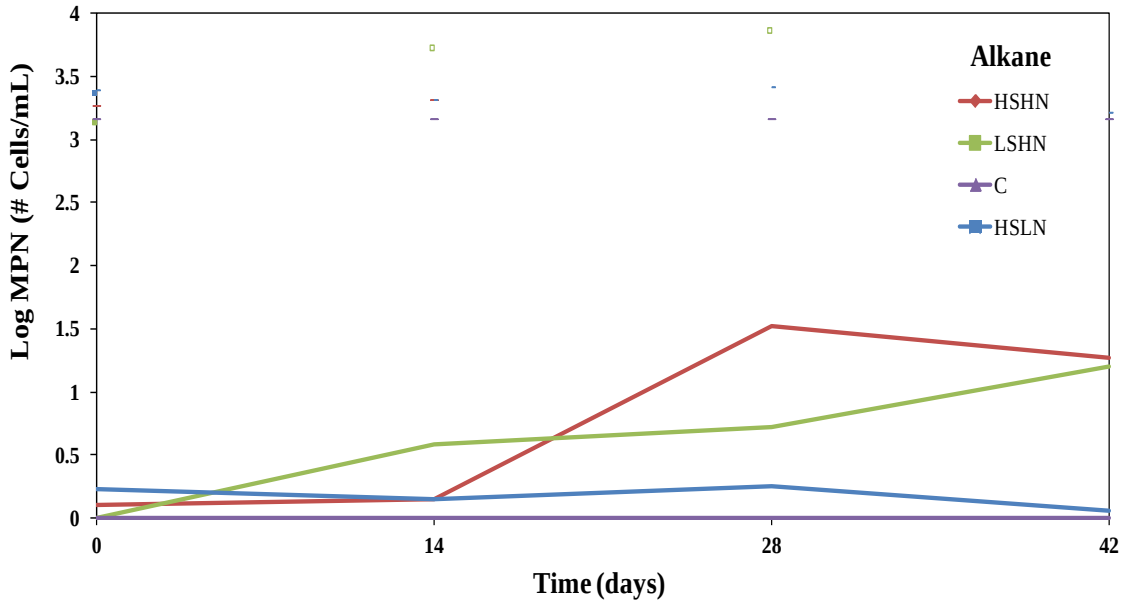

Figure 3.15 Log most probable number (MPN) of alkane degraders versus time for each of the experimental conditions.

The log MPN of heterotrophic bacteria values for each of the experimental conditions can be found in Table 3.5. The plot of the log MPN of heterotrophic bacteria versus time can be viewed in Figure 3.16. The HSHN case rises over time and finishes at a value of 2.65 cells/mL. The LSHN case has a similar trend as the HSHN, yet it does not rise as high and ends at a value of 2.07 cells/mL. The HSLN case shows the largest spike in heterotrophic bacteria when it peaks to a value of 5.09 cells/mL at time 1. The initial, large spike may be a result of the low amount of nutrient running out so the microbial population quickly spiked and then started to decrease to values below the other two experimental conditions (HSHN and LSHN). The control case has almost zero heterotrophic bacteria present, except for an amount of 0.27 cells/mL at time three. Being that sodium azide was added to these samples to kill all of the bacteria, this may be the result of human error in the lab since heterotrophic bacteria can contaminate the process during the analysis due to the presence of other items in the laboratory that are not sterile. Even though the materials and gloves were sterilized prior to use, there are numerous ways that a slight error could result in a slight positive reading for heterotrophic bacteria.

Table 3.5 Log Most Probable Number (MPN) Values for Heterotrophic Bacteria

	Log MPN (cells/mL)			
Time (days)	**HSHN**	**LSHN**	**C**	**HSLN**
0	0.37	0.83	0.00	0.38
14	2.15	0.58	0.00	5.09
28	2.49	1.91	0.03	1.76
42	2.65	2.07	0.27	1.18

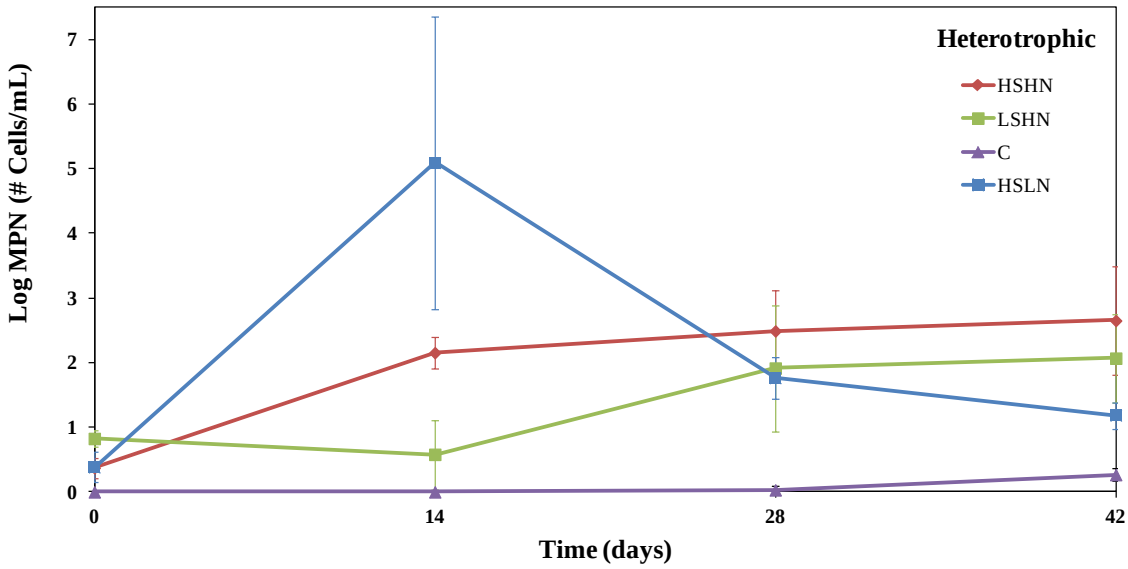

Figure 3.16 Log most probable number (MPN) of heterotrophic bacteria versus time for each of the experimental conditions.

A comparison of the TPH mass and bacterial population for the high speed, high nutrient (HSHN), low speed, high nutrient (LSHN), control (C), and high speed, low nutrient (HSLN) cases at every time point can be seen in Figures 3.17, 3.18, 3.19, 3.20, respectively. The left axis presents TPH mass (g), while the right side depicts log MPN (# cells / mL) over the course of time. These figures allow for tracking the decrease of TPH mass, along with the increase of both types of bacteria over time. As the various types of bacteria consumed the oil over time for the non-control cases, nourishment was provided to aid in microbial growth. This in turn caused an initial rise in the microbial population. After this initial period, overpopulation of microbes and limits of nutrient consumption and oil consumption cause the growth rate to slow down and then eventually stop. Note that Figure 3.19 for the control case shows almost no microbial growth due to the presence of sodium azide.

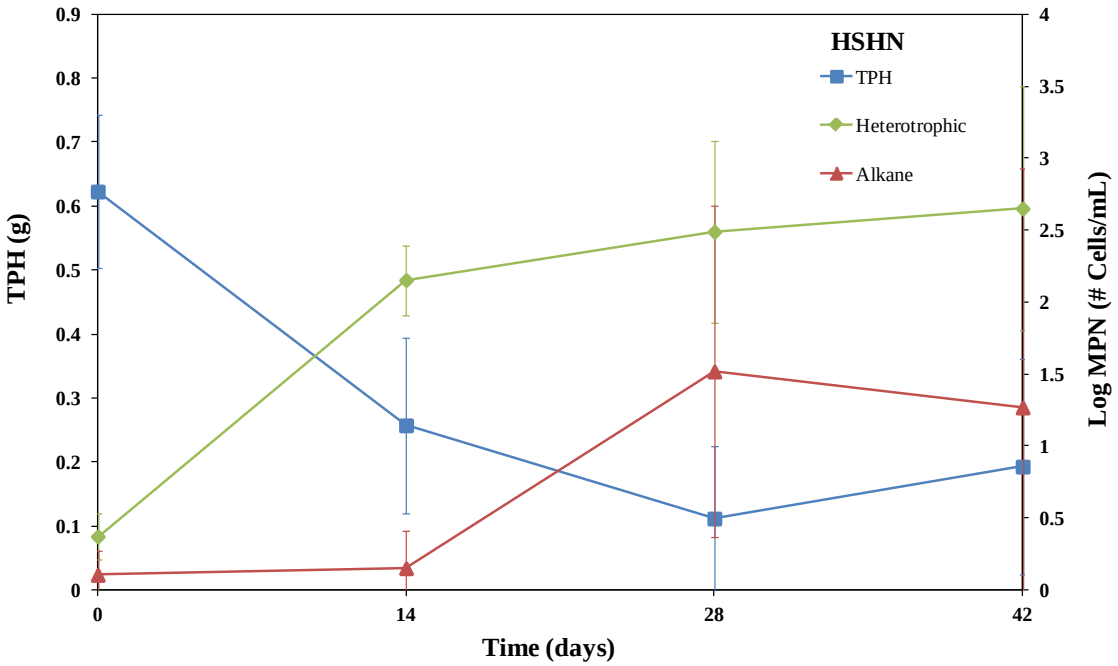

Figure 3.17 Comparison of the total petroleum hydrocarbon (TPH) mass (left axis) and most probable number (MPN) (right axis) versus time for the high speed, high nutrient case.

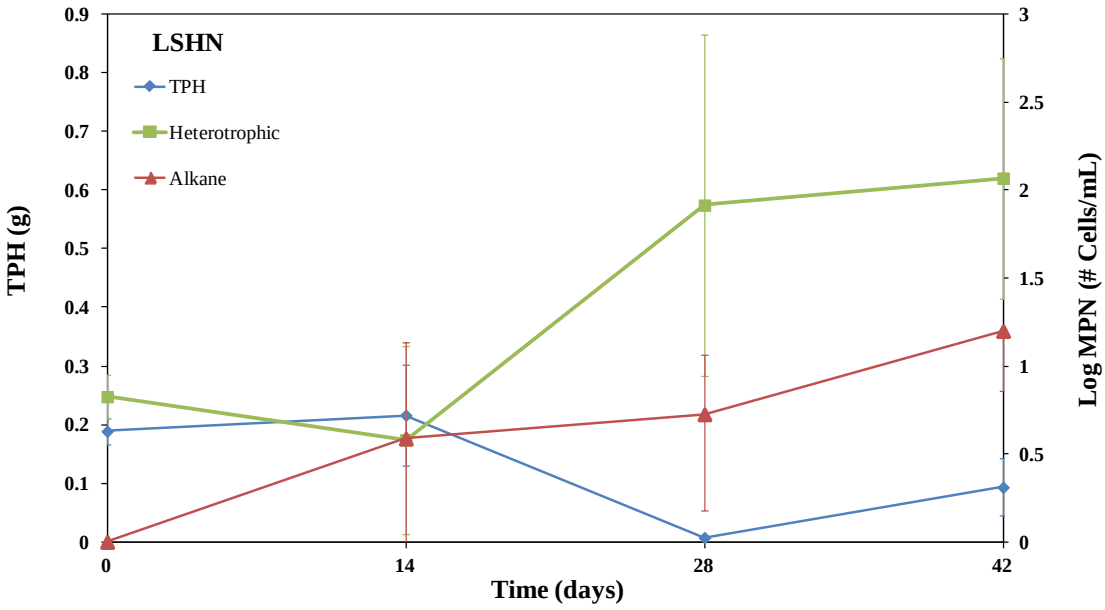

Figure 3.18 Comparison of the total petroleum hydrocarbon (TPH) mass (left axis) and most probable number (MPN) (right axis) versus time for the low speed, high nutrient case.

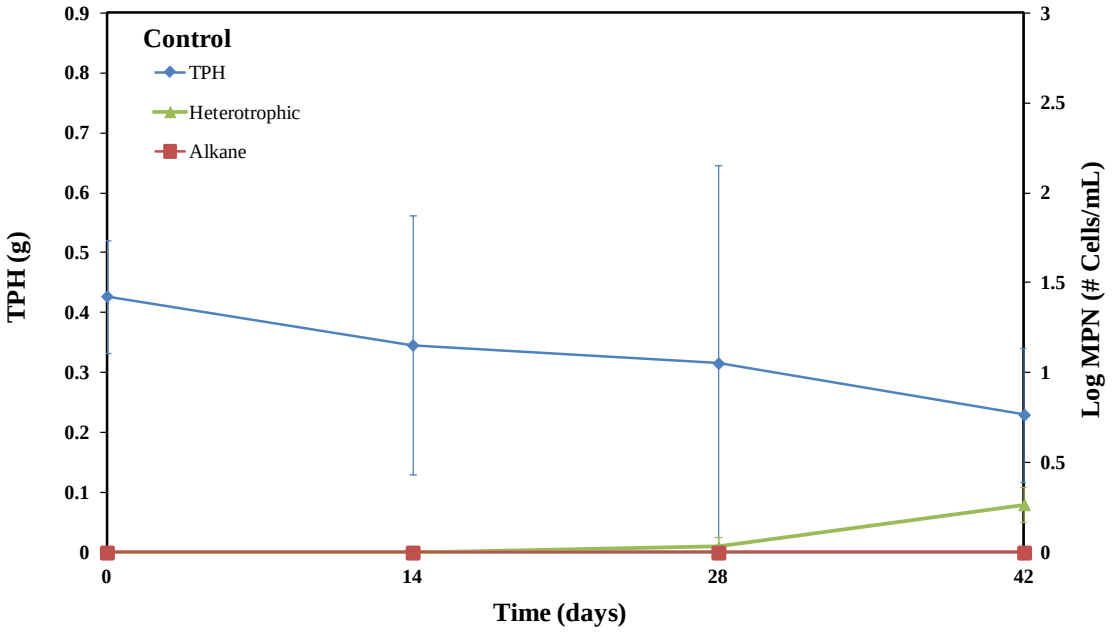

Figure 3.19 Comparison of the total petroleum hydrocarbon (TPH) mass (left axis) and most probable number (MPN) (right axis) versus time for the control case.

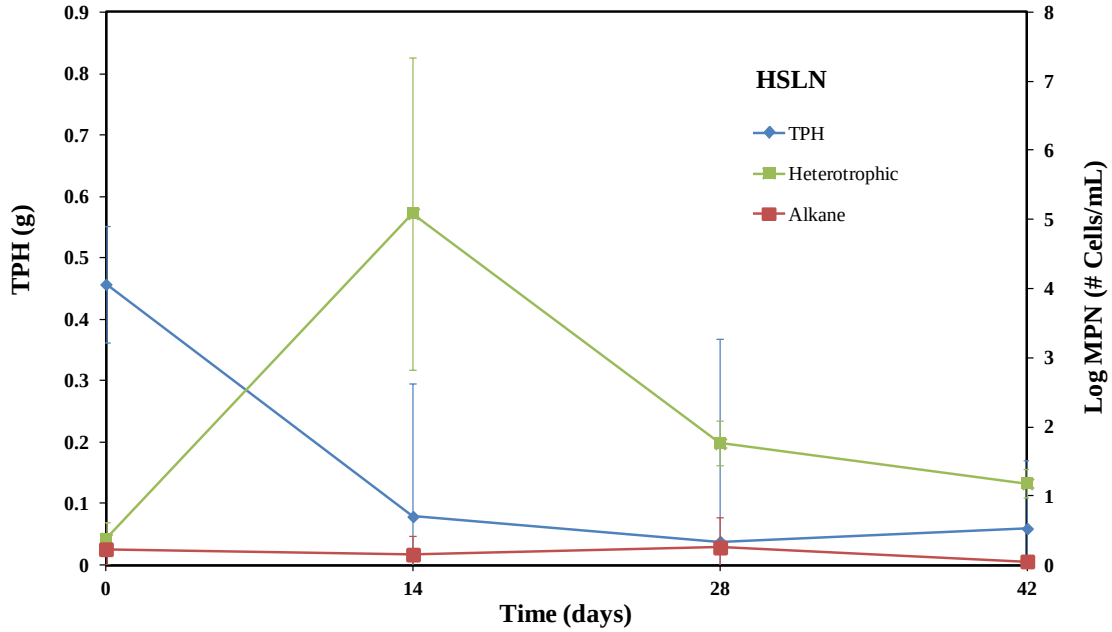

Figure 3.20 Comparison of the total petroleum hydrocarbon (TPH) mass (left axis) and most probable number (MPN) (right axis) versus time for the high speed, low nutrient case.

3.5 Oxygen Consumption and Carbon Dioxide Production

Oxygen consumption was measured routinely throughout the study and the oxygen consumption values were plotted versus time in Figure 3.21. The control condition has much lower oxygen consumption than all of the other cases, with a final cumulative value of 12.9 mg of oxygen after the 42 days. The high speed, high nutrient case has a smooth, gentle increase over time, which indicates steady oxygen consumption until it reaches a final cumulative values of 34.0 mg. The LSHN and the HSLN had oxygen consumption values that were larger than the HSHN case. There were a few instances over time, where there are uncertainties associated with the variability in the measurements as depicted by the error bars.

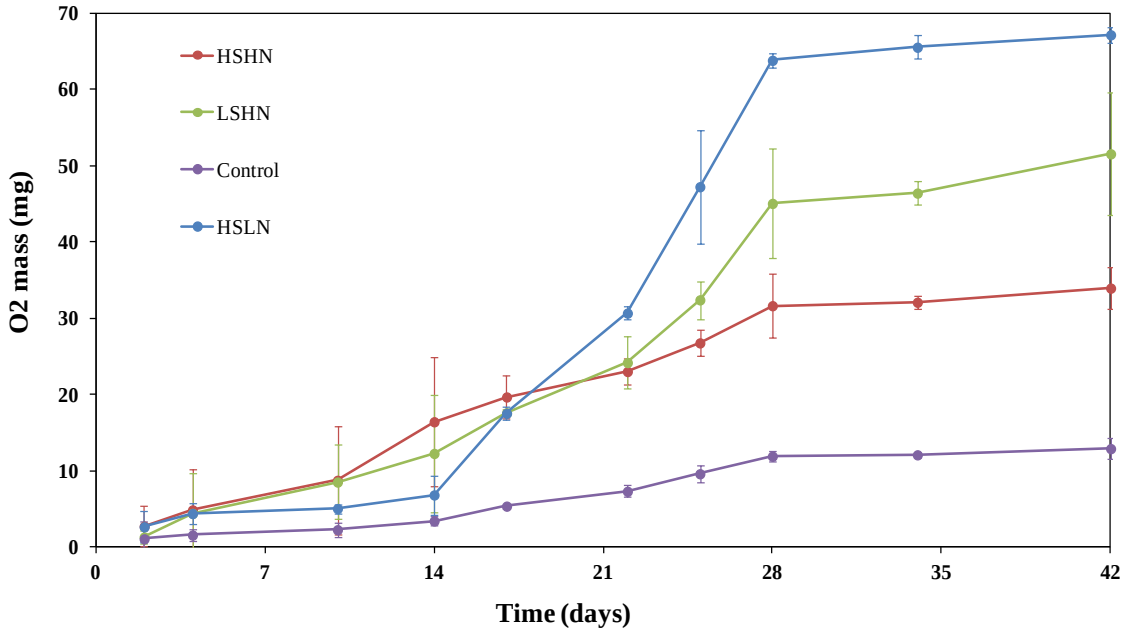

Figure 3.21 Mass of oxygen consumption versus time for each of the experimental conditions.

The plot of carbon dioxide production versus time can be found in Figure 3.22. The production of carbon dioxide was nearly 0 mg during the 6 week study for the cases

of the control and the high speed, low nutrient. The high speed, high nutrient case had a cumulative total amount of CO_2 production of 109.4 mg at time 3, whereas the low speed, high nutrient case had a final total of 99.4 mg. The HSHN values were higher than those of LSHN at each time interval, yet the CO_2 production followed a similar trend as one another.

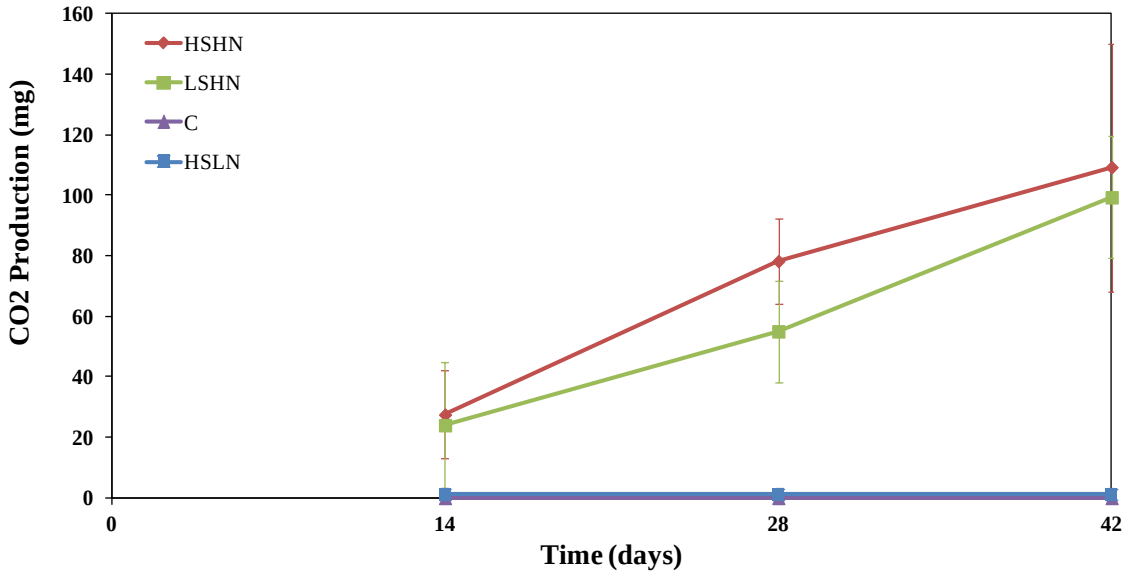

Figure 3.22 Mass of carbon dioxide production versus time for each of the experimental conditions.

3.6 Nutrient Consumption

The amount of nutrient consumption was measured over time. Nitrate and phosphate were the nutrients that were added and monitored over the course of the experiments. Nitrate concentration versus time for all of the experimental conditions can be found in Figure 3.23. Both of the high nutrient cases (HSHN and LSHN) start off with large nitrate concentrations but then plummet by time 2. This coincides with the spikes in microbial growth, which implies that the microbes are consuming all of the available nitrates during each case. There is an unusual spike in nitrate concentration for the

control at time 1, which may be an error since these values have a large standard deviation (not shown to make the plot easier to view). At time one, all of the samples have a nitrate concentration that is approximately 100 mg/L or higher. Note that these trends reflect the numbers that were obtained, but after further research, it has been determined that the actual values were subject to interference from the dispersant (Chapter 6 presents a more detailed description of this issue).

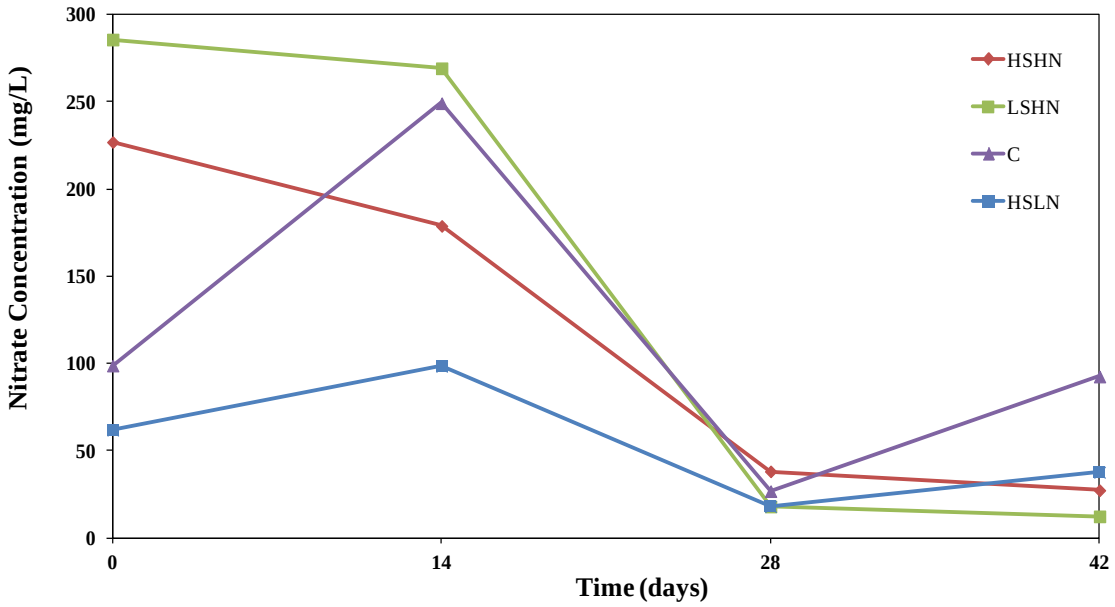

Figure 3.23 Nitrate concentrations versus time for each of the experimental conditions.

Phosphate concentration versus time for all of the experimental conditions can be found in Figure 3.24. The high nutrient samples start out with approximately 11 mg/L of phosphate and the HSHN drops to about half of the initial amount as it is used up. The LSHN case does not drop over time, yet the error bars are very large, implying large variations between the triplicates. The two low nutrient cases (C and HSLN) show low levels of phosphate for the duration of the 42 days.

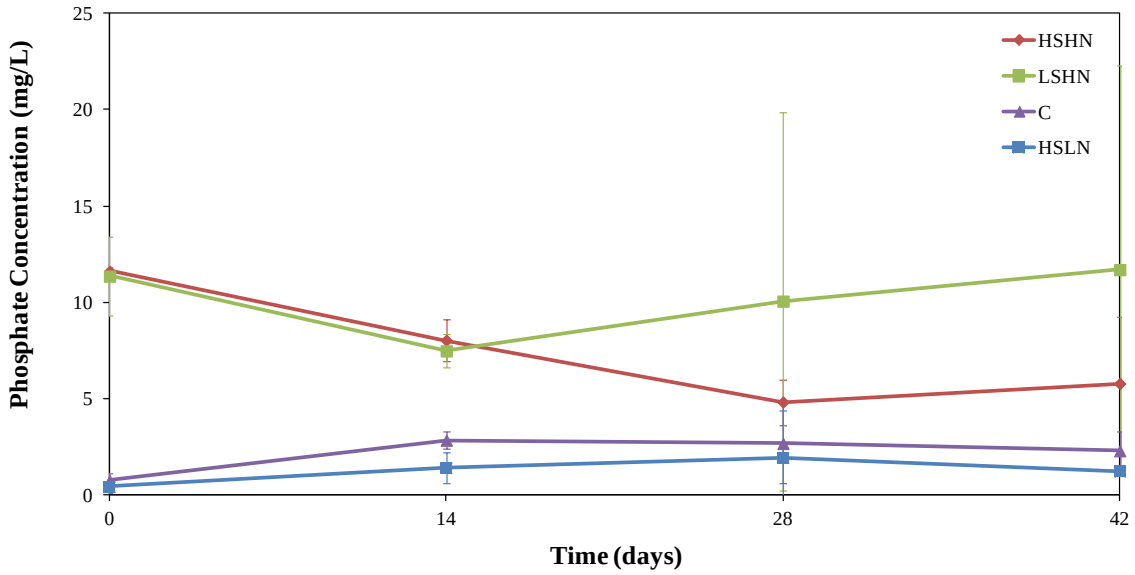

Figure 3.24 Phosphate concentrations versus time for each of the experimental conditions.

Estimated nutrient concentrations needed for the microbial growth that occurred was calculated for each case and is presented in Table 3.6. As anticipated, the largest amount of biomass increase was for the HSHN case, whereas the smallest was during the control case at values of 1.29×10^{-4} and 5.18×10^{-7} mg/L, respectively. The increases for the LSHN and the HSLN cases were 3.53×10^{-5} and 3.61×10^{-6} mg/L, respectively. Nutrient calculations were then based on the stoichiometric relationships between the nutrients and the assumed biomass formula, and the calculated trends here are in line with the trends that were viewed for most of the experimental data.

Table 3.6 Calculated Biomass Growth and Estimated Nutrient Consumption

Experimental Condition	Biomass Increase (mg/L)	Estimated Nitrogen Consumption (mg/L)	Estimated Phosphorous Consumption (mg/L)
HSHN	1.29E-04	1.56E-05	3.45E-06
LSHN	3.53E-05	4.26E-06	9.42E-07
C	5.18E-07	6.25E-08	1.38E-08
HSLN	3.61E-06	4.35E-07	9.63E-08

CHAPTER 4

DISCUSSION

The effects of mixing rates and nutrient addition on aerobic biodegradation of oil were evaluated using respirometric flasks and standard protocols as reported by literature. The presence of dispersant (Corexit 9500) for all of the experimental cases has also effectively contributed to dispersing the oil into the seawater under the applied mixing conditions, as determined by previous studies (Personna, King, Boufadel, Zhang, & Kustka, 2014). Initial oil concentrations were three times lower and the oil droplet distribution was larger when a lower mixing speed was employed. Therefore, it is easy to view the impact of mixing intensity on oil droplet diameter size and how well the oil gets distributed into the water column. The oil-water interfacial specific area becomes larger with higher mixing, thus allowing the bacteria to have easier access in order to consume the oil. Oil loss due to sticking on the glassware before the initial measurements will also impact biodegradation rate, since it is more difficult for the bacteria to remove larger quantities of oil.

It has been reported that the amount of oil and its chemical composition, and nitrogen available to microbes were among the most significant factors contribution towards biodegradation for the Exxon Valdez oil spill (Bragg, Prince, Harner, & Atlas, 1994). The nitrate concentrations in the seawater plummeted at day 28 (time 2) indicating that nitrate concentrations are a limiting factor in the biodegration rate for this study. The phosphate concentrations do not experience as large as a drop as the nitrate concentrations. For most of the conditions, the peak bacterial population coincides with the lowest amount of TPH mass at day 28.

Going back to examine the relationship between total petroleum hydrocarbon mass and most probable number count versus time in Figure 3.17, it can be seen that the high speed, high nutrient condition underwent a sharp decrease in TPH from time 0 to time 1, which accompanies a sharp increase in heterotrophic bacteria MPN and a small increase in the amount of alkane degraders over that same time span. The increasing bacterial population then continued to consume oil as the TPH continued dropping until time 2, while the heterotrophic MPN underwent a slight increase and the MPN of the alkane degraders had a large increase. It is from time 2 to time 3 that each of these values began to level off, thus indicating a steadying of the biodegradation rates.

Looking at the TPH and MPN for the low speed, high nutrient case in Figure 3.18, the curve depicts roughly no change in TPH or heterotrophic bacteria at time 1, yet an increase in alkane degraders was observed. The TPH then drastically dropped from time 1 to time 2, as the heterotrophic bacteria spikes and the alkane MPN continued to rise. After this point, the oil mass did not decrease any further and heterotrophic bacteria population also remained the same.

Exploring the relationship between TPH and MPN for the control case in Figure 3.19, it was observed that there was only a very small amount of bacterial growth over time (which may have been caused by human error in the laboratory). Therefore, the steady loss of oil was due to the physical loss of oil, including evaporation. Turning to explore the relationship addressed in Figure 3.20, the graph shows that the high speed, low nutrient case only had a low presence of alkane degraders over time. A large spike in heterotrophic bacteria occurred at time 1, which was where the largest decrease of TPH

mass occurred. The heterotrophic bacterial population decreased and the TPH oil mass for those samples does not change much from time 1 through time 3.

The biodegradation of total petroleum hydrocarbon over time follows Monod kinetics. Biomass needed time to grow to a certain level before it was able to consume oil at a faster rate. This initial lag time lasted for roughly the first ten days. After the biomass reached a peak, the oil was biodegraded very rapidly. Once most of the oil was degraded, the biomass tended to decrease, resulting in the slowdown of biodegradation rate.

Mixing speed had the greatest effects on oil biodegradation in this study. One reason is that mixing speed caused different initial oil concentrations in the water column. Lower speeds prevent the oil from being thoroughly mixed into the water column, so those initial concentrations were lower. The effects of nutrient limitation were not an obvious factor compared to mixing speed, based on the experimental data. Therefore, oil biodegradation mainly depended on the interfacial area, so the microbes had more area to consume the oil. High mixing speeds led to smaller diameters, which in turn led to larger values of interfacial specific area. For a quick example to understand these effects, assume there is an oil droplet that has a volume of one cubic micron for one case, yet for the other case, assume that there are two smaller drops that each has a volume of 0.5 cubic microns. By calculating surface area of the oil droplets for each case, it can be seen that the two smaller droplets have a surface area that is 26% larger than the case involving the single oil droplet.

CHAPTER 5

CONCLUSIONS

The impact of oil droplet size distribution and mixing energy on oil biodegradation was examined by performing a baffle flask experiment. As anticipated, the flasks that were mixed at faster speeds resulted in a smaller size distribution of oil drops. The oil droplet distribution for the lower mixing speed case showed larger droplets than the other cases. Also, over the course of the 42 day study, these drops grew over time to sizes that were larger than an order of magnitude compared to all of the other cases. The smaller droplets had greater interfacial specific area, which in turn allowed bacteria to have easier access for consuming the oil droplets. It was observed by experimentation that the droplets created from low speed mixing had an oil droplet distribution curve with smaller interfacial specific areas compared to droplets formed during the higher speed conditions.

The control case and the case with low speed mixing (LSHN) finished at time three with a total petroleum hydrocarbon mass of roughly half of their initial values for the respective trials. Compared to the two cases with high mixing and no biocide present, the peak amount of oil loss was 82% and 87% of the initial values for the HSHN and the HSLN cases, respectively. Most probable number was experimentally measured in order to study the amounts of three types of the bacteria that were present; alkane degraders, heterotrophic bacteria, and 3-ring polycyclic aromatic hydrocarbons. The control case had relatively no microbial activity due to the addition of the biocide, sodium azide. The high speed, high nutrient case had the largest amount of biomass growth compared to the other cases. Therefore, along with the presence of chemical dispersant for all of the cases,

it was determined experimentally that mixing speed was a larger factor on oil biodegradation than the addition of nutrients to the seawater.

CHAPTER 6

FUTURE WORK

After the completion of this study, it became apparent that there are certain logical areas of interest to investigate in the future to expand upon this work. One such area where future study will be required is a direct result from discovering that the UV-visible spectrophotometer gave positive readings for nitrate due to the presence of Corexit 9500, which was added to each sample. There was not any extra nutrient added to these samples, yet they showed large values of nitrate. As a test, similar oil-water samples were prepared, and the value of nitrate that was detected was negligible. However, when Corexit was added to the same samples, the values increased drastically. As an additional test, new samples were prepared with only Corexit 9500 and seawater. Large values of nitrate were detected in these samples as well. Therefore, the UVV cannot be relied upon for accurate nitrate values due to interference that was caused by the presence of Corexit. However, the trends that were measured from the UVV can give a better picture of the consumption of nitrate.

A different method of measuring the concentration of nitrate needs to be employed in the future. One potential method that can be used for detecting that actual concentration of nitrate even when Corexit 9500 is present is Fourier-transform ion cyclotron resonance mass spectrometry (FT-ICR-MS) (Seidel, Kleindienst, Dittmar, Joye, & Medeiros, 2015). Two other potential ways to measure nitrate concentration include high performance liquid chromatography (HPLC) (Shen et al., 1997) and ion chromatography (Ambrosoli, Petruzzelli, Minati, & Marsan, 2005).

The total petroleum hydrocarbon mass did not account for the oil that was left behind in the baffled flasks and microcosms. Each case, specifically the control case, had amounts of oil that were stuck onto the glassware. One way to measure this would be to rinse all of the glassware with DCM to measure the mass of the oil that was left behind in order to account for all of it.

Another potential area to explore in the future includes investigating different surfactants and different types of oil. It would be relevant to see how mixing speed and nutrient addition impacts these other materials, thus allowing us to be more prepared before the next major oil spill occurs. Another interesting area to be explored would be the role of temperature and salinity of the water on the biodegradation of dispersed oil. Finally, modeling the biodegradation of the oil for the conditions presented in this study, as well as any future studies would help expand our current knowledge of oil biodegradation.

APPENDIX

GENERAL INFORMATION ON OIL SPILLS

Oil spills have had catastrophic effects on the environment in the past. These have been some of the worst disasters that humans have had to deal with. The imagery alone is difficult to tolerate and the environmental impact can be irreversible. One such notable disastrous oil spill was the Exxon Valdez spill. In 1989, an Exxon Valdez tanker spilled its oil onto more than 1,300 miles of Alaskan coast. The Exxon Valdez Oil Spill Trustee Council reports that 11 million gallons of oil were spilled and estimated that 250,000 birds, 2,800 otters, 300 seals, 250 bald eagles, more than 20 killer whales and countless other creatures were killed as a result.

According to the National Oceanic and Atmospheric Administration (NOAA), major oil spills can have horrendous consequences on wildlife and plant life. High concentrations of oil are toxic to animals (and humans) and can kill by causing physical or biochemical harm. One such example of physical harm is when a bird gets coated in thick crude oil. This is an image that every person has ingrained in their heads after viewing news footage of major oil spills.

In the days, weeks, months, and even years following a major oil spill, hundreds of thousands of living things, including birds, otters, crabs, shellfish, coral reefs, etc., often die along with their surrounding ecosystems. The environment can get so damaged that it can even make it difficult for future animals and plants to live there.

With all of this in mind, here is a detailed description of the five largest oil spills in history:

Oil Spill Number 5: 1979 Atlantic Empress/Aegean Captain, Caribbean Sea: 90 Million Gallons of Oil Spilled (Gao, Hu, Wang, & Jiang, 2014)

On July 19, 1979, two massive oil tankers, the Atlantic Empress and the Aegean Captain, collided 10 miles off the coast of Tobago in the Caribbean Sea. Inclement weather caused by Tropical Storm Claudette caused this oceanic disaster resulting in the deaths of 26 people (AssociatedPress, 1979, July 22). This weather-based crash led to one of the largest oil spills in history.

When the ships collided, fires erupted on both of the ships. The Aegean Captain managed to contain its fire and was eventually towed back to land, while only spilling a small amount of oil as a result of the crash and ensuing fire.

The fate of the Atlantic Empress was much worse. According to Fortune, the Empress was towed further and further out to sea, leaking oil the entire way, before the flames got completely out of control leading to the explosion of the ship, and then it subsequently sank down to the bottom of the sea (AssociatedPress, 1979, August 6). In the aftermath of this crash, the Empress spilled its entire load of more than 270,000 tons of light crude oil (Burgherr, 2007).

What is even more shocking is that the nature of the accident prevented any environmental studies from being conducted on the impact of the oil spill. There were only reports surfacing of minor pollution to the Caribbean island shorelines. (Horn & Neal, 1981)) of the University of Georgia noted that an unknown amount of the oil burned on the surface of the ocean due to the fires that occurred on the ships. By August 9, 1979, the oil slick that was left behind by the Empress had already disappeared from the surface. The ship was also lost due from sinking at that time. This unfortunate incident holds the record as the largest oil tanker spill in history to this day.

Oil Spill Number 4: 1979 Ixtoc 1 Oil Spill, Bay of Campeche: 125 Million Gallons of Oil Spilled

One of the first major oil spills to impact the Gulf of Mexico occurred more than three decades ago, on June 3, 1979. This spill was located about 50 miles off the Mexican coast in the Bay of Campeche.

A blowout and resulting explosion sank the rig that was tapping into the IXTOC 1 oil well. According to NOAA, this resulted in a quantity of 10,000 to 30,000 barrels (315,000 to 945,000 gallons) of oil a day was released into the Gulf of Mexico.

The well was under the control of Pemex, which was Mexico's government-run oil company. They attempted to plug the leak after the blowout by activating the blowout preventer mechanism beneath the surface of the Gulf. However, disaster struck again. Upon activating the preventer mechanism, the pressure from the well caused some of the pipes to start rupturing oil. Therefore, that plan needed to be abandoned since it was not a viable solution. In turn, the blowout preventer mechanism was deactivated, which allowed oil to once again shoot out from the well.

They were able to successfully reduce the flow of oil by pumping mud and metal balls into the ruptured well. The Woods Hole Oceanographic Institution notes that the more than 125 million gallons of oil still spilled into the water for a duration of nearly 10 months (Patton, Rigler, Boehm, & Fiest, 1981). Adding to this unfortunate event was the presence of high winds to the north, which carried a 300 foot-by-500 foot oil slick onto the Texas coastline. NOAA reported that the entire coastline of south Texas had experienced some degree of oil as a result of this spill. Roughly 162 miles of U.S. coastline was impacted by a quantity of 71,500 barrels (2,252,250 gallons) worth of the oil (ERCO, Energy Resources Co. Inc., 1982).

Eventually, two relief wells were drilled around IXTOC 1. These were able to effectively slow the flowing oil enough to allow the capping of the well to occur on March 23, 1980 (U.S.DOI/MMS, U.S. Dept of Interior/ Minerals Management Service, 1982).

The BBC reports that the full extent of the environmental impact is hard to gauge. There have even been discrepancies amongst various research studies on the spill. One research study argued that the impact was small, yet another argued that it was quite extensive (R.M. Atlas, 1981). NOAA notes that the Mexican government vehemently argued that the spill caused limited impacts and that the oil was either burned up, evaporated or collected as a result of the containment efforts.

Fisheries along the coast in the Mexican state of Campeche have suffered greatly resulting in many to be shut down. The Times-Picayune reports that the Mexican government is still handing out compensatory damages to the fisherman in that area. The yearly financial totals add up to nearly $800,000.

There is the same amount of uncertainty about the spill's environmental impact on U.S. soil, but the U.S. Fish and Wildlife Service (USFWS) recovered more than 1,400 oiled birds (Romero, Harvey, & Atwood, 1981). In a surprising bit of good news, NOAA reported that a tropical system helped with the removal of up to 80 percent of oil from the U.S. coast in September of 1979.

Oil Spill Number 3: 2010 B.P. Oil Spill, Gulf of Mexico: 200 Million Gallons of Oil Spilled

On April 20, 2010, an explosion occurred on the Deepwater Horizon drilling platform. The location of this explosion was roughly 50 miles off the coast of Louisiana in the Gulf

of Mexico. This led to the worst oil spill in U.S. history. Unfortunately, there were casualties as a result of the explosion. Eleven Deepwater Horizon workers died, while another 17 were seriously injured. The Times Picayune reports that the rig burned for two days before it suck to the bottom of the Gulf of Mexico.

There was a federal investigation conducted by the U.S. Chemical Safety Board. They concluded that the blowout could have been prevented if a blowout preventer mechanism on the Horizon did not fail. However, the mechanism's failure resulted in more than 200 million gallons exiting the well at a depth of 5,000 feet below the water surface, for a duration of 87 days (Sammarco et al., 2013).

This technically was not the largest oil spill in U.S. history (the largest will be discussed in the pages to follow). However, the amount of environmental damage makes many people consider the Deepwater Horizon spill to be the worst spill in human history.

The Smithsonian National Museum of Natural History reports that the oil floated to the surface, forming a 5,000-square-mile oil slick that was pushed ashore along the Gulf Coast by a combination of winds and currents. This resulted in all of the observable features that are synonymous with major oil spills, such as birds that are drenched in oil and beaches that are littered with tarballs. After only four months after the spill, the New York Times reported that an astonishing amount of at least 7,000 birds, sea turtles and dolphins were found dead or crippled as a direct result of this spill.

The Natural Resource Damage Assessment (NRDA) report was a federal effort to determine a definitive figure on the total impact of the spill. However, this report has not been completed yet. NOAA explains that such a report is difficult to create due to the geographic size, three-dimensional aspect of the spill, and the ecological complexity.

They also added that these factors make it the largest assessment ever carried out by the agency. Therefore, it is unlikely that a final quantitative value will be released for many years to come. From the time of the spill in 2010 until today independent research projects that were conducted anticipate the quantity of animal deaths to be magnitudes greater than the initially 7,000 figure which was quoted by the New York Times. For example, one study was performed and the researchers estimated that a total amount of around 800,000 birds were killed as a result of the spill (Haney, Geiger, & Short, 2014).

There are other potential impacts that can result from a major oil spill such as this one. A 2012 NOAA study linked the oil spill to a hormone deficiency in bottlenose dolphins in the Gulf of Mexico. This deficiency caused the dolphins to be to emaciated and sickly. That deficiency contributed in part to the deaths of more than 900 dolphins since the start of the spill (Dell'Amore, 2014). NOAA reports that more than 600 sea turtles have been found dead since the oil spill. Only 18 of them were visibly covered in oil which implies that their natural environment was ruined due to the oil.

There are potential long term effects on the wildlife according to a recent report by the National Wildlife Federation, which is an environmental advocacy group. This report indicates that 14 species of animals were still suffering adversely from oil spill-related impacts.

The environmental impacts are more extensive than anticipated when considering the massing amount of the oil that did not even reach the surface. Large oil plumes remained suspended in the ocean and some of these plumes even sank down to the floor of the ocean. A recent study that was performed by the National Academy of Sciences discovered that a 1,200 square mile "bathtub ring" of oil happened to settle on

the sea floor around the drill site (Valentine et al., 2014). Therefore, deep sea creatures, organisms, and ecosystems have probably also been severely impacted by the spill. Further research is needed to quantify the full extent of the underwater damage that resulted from the spill. One study did conclude that there were adverse impacts on the deepwater ecosystems around the well that will take decades to recover (Montagna et al., 2013). Regardless of the findings of all of these future studies, there is no oil spill in recent history that matches the scale and environmental impact of the Deepwater Horizon spill. One must hope that this remains the case well into the future by implementing the proper protocols and potential responses to prevent all future spills.

Oil Spill Number 2: 1991 Gulf War Oil Spill, Persian Gulf: 240 Million-336 Million Gallons of Oil Spilled

As strange as it sounds, one of the largest oil spills in history was not accidental. It turns out that it was an act of war. As part of a strategy to slow down the advancing U.N. Coalition Forces, Iraqi troops whom were occupying Kuwait during the Gulf War intentionally destroyed oil tankers, wells and other oil infrastructure in January 1991.

The National Oceanic and Atmospheric Administration (NOAA) reports that an estimated 25 million gallons-plus (8 million barrels) (NOAA/HMRAD, National Oceanic and Atmospheric Administration/ Hazardous Materials Response and Assessment Division, 1992) of oil flowed off Kuwait and directly into the Arabian Gulf (Al-Lihaibi & Ghazi, 1997). This created an oil slick off the coast that was 600 square miles in size. A quantity of more than four hundred miles of coast was soiled with oil and tarmats up to 12 inches thick.

Since this was an act of war and there was an active war going on around the spill, the cleanup response was very slow. The major efforts of cleaning up this spill were not really started until about a month after the war ended. More than a million barrels of oil had been removed from the Arabian Gulf by April of 1991.

An estimated 20,000 dead birds and countless dead crabs are part of the known environmental impact. Over a decade later, plant life in the region, particularly in marshes, were struggling to recover from the devastating effects of the spill (Jones, Plaza, Watt, & Al Sanei, 1998), (Readman et al., 1998). There have also been recent recovery projects to help revive the struggling ecosystem (Michel & Rutherford, 2013). Unfortunately, it seems that there may be other environmental impacts that are still not known at this point in time.

Oil Spill Number 1: 1910 Lakeview Gusher, Kern County, California: 378 Million Gallons of Oil Spilled

Despite the lack of notoriety, the largest oil spill in world history occurred on U.S. soil back in1910 in Kern County California. The U.S. Geological Survey (USGS) describes that how, back in the late 19th and early 20th centuries, a lack of effective technology led to gushers at new oil wells (Takahashi & Gautier, 2007). These gushers were uncontrolled, towering columns of oil that shot out of the ground, generally for weeks or more at a time. Gushers led to many negative results despite just the dumping of immense amounts of oil onto the surrounding environment. They also sparked fires, destroyed oil equipment, and in some instances, even killed oil workers**,** (Gillis, 2010).

Eventually pressure control systems were developed by the oil industry, which led to the disappearance of gushers as a common practice. However, before this was done,

the Lakeview Gusher dumped 378 million gallons of crude oil onto a region in California that is less than 100 miles north of Los Angeles. The Lakeview 1 well, which was the name of the site of the gusher, did not produce oil for more than 14 months. This lack of productivity led to the oil company that was in charge of the site ordering the workers give up and stop drilling.

There was a delay in communication, so workers were still there boring into the ground on March 14, 1910. They bore into the ground and then the well erupted. This sent a 20-foot-wide, 220-foot-high column of oil into the sky over California (CRB/CSL, California Research Bureau/ California State Library) (2010). The height of the gusher was visible from more than 30 miles away according to the USGS. The well infrastructure was completely destroyed and a huge crater was left in the ground. It was estimated that an estimated amount of 125,000 barrels (3.9 million gallons) of oil a day erupted from the ground (Harvey, 2010)**.**

The oil was flowing at nearly the same rate 30 days later, at around 90,000 barrels a day, which continued for more than 17 months. A total quantity of 378 million gallons worth of oil flowed from the geyser. Despite less than half of the crude oil being collected, the USGS notes that this gusher single-handedly lowered the global price of crude oil. The millions of gallons of oil formed a river that was 8 miles long. This was a direct environmental threat to the nearby Buena Vista Lake, and the local the water supply. Therefore, as an attempt to contain the spill, construction crews dug out 20 pits to contain the oil. Some of these pits were so deep, that they could only be crossed via boat.

These same pits that were used to contain he oil spill would lead to the demise of the great gusher. The pits caused the oil to get backed up and pool around and over the

gusher. The flow would then fall back into the hole. After a while, the drill hole collapsed and the gusher ceased to exist (Gleeson, 2010). Oil that was unable to be collected ended up seeping back into the ground and evaporated. More than a century later, there is very little sign of what the environmental impacts of the spill were on that area. Today, the remains of Lakeview can be visited and there is a plaque on the site, although the plaque fails to effectively illustrate the largest oil spill in recorded history.

REFERENCES

Al-Lihaibi, S. S., & Ghazi, A. J. (1997). Hydrocarbon Distributions in Sediments of the Open Area of the Arabian Gulf following the 1991 Gulf War Oil Spill. *Mar Pollut Bull, 34*(11), 8. doi: 10.1016/S0025-326X(97)00069-6.

Ambrosoli, R., Petruzzelli, L., Minati, J. L., & Marsan, F. A. (2005). Anaerobic PAH Degradation in Soil by a Mixed Bacterial Consortium Under Denitrifying Conditions *Chemosphere, 60*, 7.

AssociatedPress. (1979, August 6). Supertanker's Sinking May Set Record Loss, *The Virgin Islands Daily News*. Retrieved from http://news.google.com/newspapers?id=rRBOAAAAIBAJ&sjid=Eq4DAAAAIBAJ&pg=6043,706069&dq=atlantic+empress&hl=en. Accessed February 10, 2015.

AssociatedPress. (1979, July 22). Crippled Tankers Spill More Oil, *The Sunday Star News*. Retrieved from http://news.google.com/newspapers?id=K7YsAAAAIBAJ&sjid=MBMEAAAAIBAJ&pg=5888,4568782&dq=atlantic+empress&hl=en. Accesed February 10, 2015.

Atlas, R. M. (1981). Fate of Oil from Two Major Oil Spills: Role of Microbial Degradation in Removing Oil from the Amoco Cadiz and IXTOC I Spills. *Environmental International, 5*(1), 6. doi: 10.1016/0160-4120(81)90111-2.

Atlas, R. M., & Bartha, R. (1973). Stimulated biodegradation of oil slicks using oleophilic fertilizers. *Environ. Sci. Technol., 7*(6), 538-541.

Bælum, J., Borglin, S., Chakraborty, R., Lamendella, R., Auer, M., Conrad, M. E., . . . Jansson, J. K. (2012). Deep-sea Bacteria Enriched by Oil and Dispersant from the Deepwater Horizon Spill. *Environ Micobio, 14*(9), 12. doi: doi:10.1111/j.1462-2920.2012.02780.x.

Blondina, G. J., Singer, M. M., Lee, I., Ouana, M. T., Hodgins, M., Tjeerdema, R. S., & Sowby, M. L. (1999). Influence of Salinity on Petroleum Accommodation by Dispersants. *Spill Science and Technology Bulletin, 5*(2), 8.

Boufadel, M. C., Reeser, P., Suidan, M. T., Wrenn, B. A., Cheng, J., Du, X., . . . Venosa, A. D. (1999). Optimal nitrate concentration for the biodegradation of n-heptadecane in a variably-saturated sand column. *Environ. Technol., 20*(2), 191-199.

Boufadel, M. C., Sharifi, Y., Van Aken, B., Wrenn, B. A., & Lee, K. (2010). Nutrient and oxygen concentrations within the sediments of an Alaskan beach polluted with the *Exxon Valdez* oil spill. *Environ. Sci. Technol., 44*(19), 7418-7424.

Bragg, J. R., Prince, R. C., Harner, E. J., & Atlas, R. M. (1994). Effectiveness of bioremediation for the Exxon Valdez oil spill. *Nature, 368*(6470), 413-418.

Burgherr, P. (2007). In-depth Analysis of Accidental Oil Spills from Tankers in the Context of Global Spill Trends from All Sources. *J Hazard Mater, 140*(1-2), 245-256. doi: 10.1016/j.jhazmat.2006.07.030.

Camilli, R., Di Iorio, D., Bowen, A., Reddy, C. M., Techet, A. H., Yoerger, D. R., . . . Fenwick, J. (2012). Acoustic measurement of the Deepwater Horizon Macondo well flow rate. *P. Natl. Acad. Sci. USA, 109*(50), 20235-20239.

Campo, P., Venosa, A. D., & Suidan, M. T. (2013). Biodegradability of Corexit 9500 and Dispersed South Louisiana Crude Oil at 5 and 25°C. *Environ Sci Technol, 47*, 8.

CRB/CSL. (California Research Bureau/ California State Library) (2010). *Studies in the News: California - One Hundred Years Ago*. Retrieved from http://www.library.ca.gov/sitn/crb/docs/20100629.pdf. Accessed February 10, 2015.

Dell'Amore, C. (2014). Gulf Oil Spill "Not Over": Dolphins, Turtles Dying in Record Numbers. National Geographic News. Retrieved from http://news.nationalgeographic.com/news/2014/04/140408-gulf-oil-spill-animals-anniversary-science-deepwater-horizon-science/. Accessed February 10, 2015.

Dou, J., Liu, X., Hu, Z., & Deng, D. (2008). Anaerobic BTEX Biodegradation Linked to Nitrate and Sulfate Reduction. *J Hazard Mater, 151*(2-3), 720-729. doi: 10.1016/j.jhazmat.2007.06.043.

Du, X., Reeser, P., Suidan, M. T., Huang, T., Moteleb, M., Boufadel, M. C., & Venosa, A. D. (1999). *Optimum nitrogen concentration supporting maximum crude oil biodegradation in microcosms.* Paper presented at the International Oil Spill Conference.

EPA. (1996). *Method 3510C: Separatory Funnel Liquid–liquid Extraction*. (Revision 3).

ERCO. (Energy Resources Co. Inc., 1982). IXTOC Oil Spill Assessment: Final Report.

Fisher, S. D. (2005). Enhanced Biodegradation of Highly Weathered Crude Oil by Chemical Oxidation.

Gao, Z., Hu, Z., Wang, G., & Jiang, Z. (2014). An Analytical Method of Predicting the Response of FPSO Side Structures to Head-on Collision. *Ocean Engineering, 87*, 121-135. doi: 10.1016/j.oceaneng.2014.05.016.

Garrett, R. M., Pickering, I. J., Haith, C. E., & Prince, R. C. (1998). Photooxidation of crude oils. *Environmental science & technology, 32*(23), 3719-3723.

Geng, X., Boufadel, M. C., Personna, Y. R., Lee, K., Tsao, D., & Demicco, E. D. (2014). BioB:a mathematical model for the biodegradation of low solubility hydrocarbons. *Mar. Pullut. Bull., 83*, 138-147.

Gillis, J. (2010, June 21). The Era of the Oil Gusher, *The New York Times*. Retrieved from http://green.blogs.nytimes.com/2010/06/21/the-era-of-the-oil-gusher/?_r=0. Accessed February 10, 2015.

Gleeson, G. (2010). Lakeview Gusher Still Largest U.S. Oil Spill. http://abc7.com/archive/7526645/. Accessed February 10, 2015.

Haney, J. C., Geiger, H. J., & Short, J. W. (2014). Bird Mortality from the Deepwater Horizon Oil Spill. I. Exposure Probability in the Offshore Gulf of Mexico. *Marine Ecology Progress Series, 513*, 225-237. doi: 10.3354/meps10991.

Harvey, S. (2010, June 13). California's Legendary Oil Spill, *L.A. Times*. Retrieved from http://articles.latimes.com/2010/jun/13/local/la-me-then-20100613. Accessed February 10, 2015.

Head, I. M., Jones, D. M., & Röling, W. F. (2006). Marine microorganisms make a meal of oil. *Nat. Rev. Microbiol., 4*(3), 173-182.

Horn, S. A., & Neal, P. (1981). The Atlantic Empress Sinking—A Large Spill Without Environmental Disaster. *International Oil Spill Conference Proceedings, 1981*, 7. doi: http://dx.doi.org/10.7901/2169-3358-1981-1-429.

Jones, D. A., Plaza, J., Watt, I., & Al Sanei, M. (1998). Long-term (1991-1995) Monitoring of the Intertidal Biota of Saudi Arabia after the 1991 Gulf War Oil Spill. *Mar Pollut Bull, 36*(6), 18. doi: 10.1016/S0025-326X(98)00009-5.

Kaku, V. J., Boufadel, M. C., & Venosa, A. D. (2006). Evaluation of mixing energy in laboratory flasks used for dispersant effectiveness testing. *J. Environ. Eng., 132*(1), 93-101.

McGenity, T. J. (2014). Hydrocarbon biodegradation in intertidal wetland sediments. *Curr. Opin. Biotech., 27*, 46-54.

Michel, J., & Rutherford, N. (2013). Oil Spills in Marshes: Planning and Response Considerations. *NOAA/API*.

Mille, G., Almallah, M., Bianchi, M., van Wambeke, F., & Bertrand, J. C. (1991). Effect of Salinity on Petroleum Biodegradation. *Fresenius' Journal of Analytical Chemistry, 339*(10), 4.

Montagna, P. A., Baguley, J. G., Cooksey, C., Hartwell, I., Hyde, L. J., Hyland, J. L., . . . Rhodes, A. C. E. (2013). Deep-Sea Benthic Footprint of the Deepwater Horizon Blowout. *PLOS One*. doi: 10.1371/journal.pone.0070540.

Mukherjee, B., & Wrenn, B. A. (2013). Size distribution as a measure of dispersant performance. *J. Environ. Eng. Sci., 8*(1), 98-107.

NOAA/HMRAD. (National Oceanic and Atmospheric Administration/ Hazardous Materials Response and Assessment Division, 1992). Oil Spill: 1967-1991. Summaries of Significant US and International Spills *NOAA/ Hazardous Materials Response and Assessment Division*.

Oh, Y.-S., Sim, D.-S., & Kim, S.-J. (2003). Effectiveness of bioremediation on oil-contaminated sand in intertidal zone. *J. Microbio. Biotechnol., 13*(3), 437-443.

Patton, J. S., Rigler, M. W., Boehm, P. D., & Fiest, D. L. (1981). Ixtoc 1 Oil Spill: Flaking of Surface Mousse in the Gulf of Mexico. *Nature, 290*, 4.

Personna, Y. R., King, T., Boufadel, M. C., Zhang, S., & Kustka, A. (2014). Assessing Weathered Endicott Oil Biodegradation in Brackish Water. *Mar Pollut Bull, 86*(1-2), 9. doi: doi:10.1016/j.marpolbul.2014.07.037.

Prince, R. C., McFarlin, K. M., Butler, J. D., Febbo, E. J., Wang, F. C., & Nedwed, T. J. (2013). The primary biodegradation of dispersed crude oil in the sea. *Chemosphere, 90*(2), 521-526.

Readman, J. W., Bartocci, J., Tolosa, I., Fowler, S. W., Oregioni, B., & Abdulraheem, M. Y. (1998). Recovery of the Coastal Marine Environment in the Gulf Following the 1991 War-Related Oil Spills. *Mar Pollut Bull, 32*(6), 6. doi: 10.1016/0025-326X(95)00227-E.

Rittman, B. E., & McCarty, P. L. (2001). *Environmental Biotechnology: Principles and Applications*: McGraw-Hill.

Romero, G. C., Harvey, G. R., & Atwood, D. K. (1981). Stranded Tar on Florida Beaches: September 1979–October 1980. *Mar Pollut Bull, 12*(8), 5. doi: 10.1016/0025-326X(81)90452-5.

Roychoudhury, A. N., & McCormick, D. W. (2006). Kinetics of Sulfate Reduction in a Coastal Aquifer Contaminated with Petroleum Hydrocarbons. *Biogeochemistry, 81*(1), 17-31. doi: 10.1007/s10533-006-9027-5.

Sammarco, P. W., Kolian, S. R., Warby, R. A., Bouldin, J. L., Subra, W. A., & Porter, S. A. (2013). Distribution and Concentrations of Petroleum Hydrocarbons Associated with the BP/Deepwater Horizon Oil Spill, Gulf of Mexico. *Mar Pollut Bull, 73*(1), 129-143. doi: 10.1016/j.marpolbul.2013.05.029.

Seidel, M., Kleindienst, S., Dittmar, T., Joye, S. B., & Medeiros, P., M. (2015). Biodegradation of Crude Oil and Dispersants in Deep Seawater from the Gulf of Mexico: Insights from Ultra-high Resolution Mass Spectrometry. *Deep Sea Research Part II: Topical Studies in Oceanography*. doi: doi:10.1016/j.dsr2.2015.05.012.

Sharifi, Y., Van Aken, B., & Boufadel, M. C. (2011). The effect of pore water chemistry on the biodegradation of the Exxon Valdez oil spill. *Water Qual., Expo. Health, 2*(3-4), 157-168.

Shen, J., Chen, Y., Wu, S., Wu, H., Liu, X., Sun, X., . . . Wang, L. (1997). Enhanced Pyridine Biodegradation Under Anoxic Condition: The Key Role of Nitrate as the Electron Acceptor. *Chemical Engineering Journal, 277*, 10. doi: doi:10.1016/j.cej.2015.04.109.

Smith, J., Dore, S., Pope, D., Balba, T., & Weston, A. (2007, 01-15-2010). *Biodegradation Of Weathered Oil In Soils With A Long History Of TPH Contamination.* Paper presented at the Proceedings of the Annual International Conference on Soils,Sediments, Water and Energy.

Smith, V. H., Graham, D. W., & Cleland, D. D. (1998). Application of resource-ratio theory to hydrocarbon biodegradation. *Environ. Sci. Technol., 32*(21), 3386-3395.

Takahashi, K. I., & Gautier, D. L. (2007). *Petroleum Systems and Geologic Assessment of Oil and Gas in the San Joaquin Basin Province, California*. U.S. Geological Survey Professional Paper.

Torlapati, J., & Boufadel, M. C. (2014). Evaluation of the biodegradation of Alaska North Slope oil in microcosms using the biodegradation model BIOB. *Front. Microbiol., 5*, 1-15.

U.S.DOI/MMS. (U.S. Dept of Interior/ Minerals Management Service, 1982). *Third Annual Gulf of Mexico Information Transfer Meeting*.

Valentine et al. (2014). Fallout Plume of Submerged Oil from Deepwater Horizon. *PNAS, 111*(45), 6. doi: 10.1073/iti4514111.

Venosa, A., Suidan, M., Wrenn, B., Strohmeier, K., Haines, J., Eberhart, B., . . . Holder, E. (1996). Bioremediation of an Experimental Oil Spill on the Shoreline of Delaware Bay. *Environ. Sci. Technol., 30*, 12.

Venosa, A. D., & Holder, E. L. (2007). Biodegradability of Dispersed Crude Oil at Two Different Temperatures. *Mar Pollut Bull, 54*(5), 9.

Venosa, A. D., & Holder, E. L. (2013). Determining the dispersibility of South Louisiana crude oil by eight oil dispersant products listed on the NCP Product Schedule. *Mar. Pullut. Bull., 66*(1), 73-77.

Weiner, J. M., & Lovley, D. R. (1998). Anaerobic Benzene Degradation in Petroleum-contaminated Aquifer Sediments After Inoculation with a Benzene-oxidizing Enrichment. *Appl. Environ. Microbiol, 64*, 4.

Wrenn, B. A., & Venosa, A. D. (1996). Selective enumeration of aromatic and aliphatic hydrocarbon degrading bacteria by a most-probable-number procedure. *Canadian Journal of Microbiology, 42*(3), 252-258.

Yakimov, M. M., Timmis, K. N., & Golyshin, P. N. (2007). Obligate oil-degrading marine bacteria. *Curr. Opin. Biotech., 18*(3), 257-266.

Zahed, M. A., Aziz, H. A., Isa, M. H., Mohajeri, L., & Mohajeri, S. (2010). Optimal conditions for bioremediation of oily seawater. *Bioresour. Technol., 101*(24), 9455-9460.

Zhao, L., Boufadel, M. C., Socolofsky, S. A., Adams, E., King, T., & Lee, K. (2014). Evolution of droplets in subsea oil and gas blowouts: Development and validation of the numerical model VDROP-J. *Mar. Pullut. Bull., 83*, 58-69.

Zhao, L., Torlapati, J., Boufadel, M. C., King, T., Robinson, B., & Lee, K. (2014). VDROP: a numerical model for the simulation of droplet formation from oils of various viscosities. *Chem. Eng. J., 253*, 93-106.